

# Quasars: a supermassive rotating toroidal black hole interpretation

Robin J. Spivey<sup>\*</sup>

Accepted 2000 March 24. Received 2000 March 15; in original form 1999 March 18

## ABSTRACT

A supermassive rotating toroidal black hole (TBH) is proposed as the fundamental component of quasars and other jet-producing active galactic nuclei. Rotating proto-galaxies gather matter from the central gaseous region leading to the birth of massive toroidal stars, the internal nuclear reactions of which proceed very rapidly. Once the nuclear fuel is spent, gravitational collapse produces a slender TBH remnant. Transitory electron and neutron degeneracy stabilised collapse phases, although possible, are unlikely owing to the large masses involved thus these events are typically the first supernovae of the host galaxies. Given time, the TBH mass increases through continued accretion by several orders of magnitude, the event horizon swells whilst the central aperture shrinks. The difference in angular velocities between the accreting matter and the TBH induces a magnetic field that is strongest in the region of the central aperture and innermost ergoregion. Due to the presence of negative energy states when such a gravitational vortex is immersed in an electromagnetic field, circumstances are near ideal for energy extraction via non-thermal radiation including the Penrose process and superradiant scattering. This establishes a self-sustaining mechanism whereby the transport of angular momentum away from the quasar by relativistic bi-directional jets reinforces both the modulating magnetic field and the TBH/accretion disc angular velocity differential. Continued mass-capture by the TBH results in contraction of the central aperture until the TBH topology transitions to being spheroidal, extinguishing quasar behaviour. Similar mechanisms may be operating in microquasars, supernovae and sources of recurrent gamma-ray bursts when neutron density or black hole tori arise. In certain circumstances, long-term TBH stability can be maintained by a negative cosmological constant, otherwise the classical topology theorems must somehow be circumvented. Preliminary evidence is presented that Planck-scale quantum effects may be responsible.

**Key words:** black hole physics – stars: neutron – supernovae: general – galaxies: active – quasars: general – gamma-rays: bursts.

## 1 INTRODUCTION

The commonly cited method of producing ultra-relativistic bi-directional jets as observed in quasars is the mechanism described by Blandford & Znajek (1978), whereby magnetic field lines thread the poles of a rotating BH as they descend towards the event horizon. Rotational energy may be extracted from the BH by this technique which is ejected in the form of radiation and matter travelling at high velocity along the BH's spin axis. Critical assessments by Ghosh & Abramowicz (1997) and Livio, Ogilvie & Pringle (1999) suggest that the role of the Blandford-Znajek mechanism has been generally overestimated and inadequately accounts for

the larger double radio lobe structures. Numerical simulations indicate that the observed gamma ray energy release along quasar jets is four orders of magnitude more energetic than the Blandford-Znajek mechanism predicts. Issues that are difficult to reconcile with this model are the variability of jet dispersion angles, the finite quasar lifetime and the multiplicity of red-shifts in the very metallic absorption spectra. Any viable alternative model must simultaneously cater for all features.

Speculation concerning the fundamental processes governing quasars invariably involves discussion of compact massive central bodies, the consensus being that these are rotating spheroidal BHs of mass  $10^6$ – $10^9 M_{\odot}$ . Profiles of stellar orbital velocities within AGN haloes lend weight to the premise that massive objects reside at the galactic nuclei. Inactive galactic nuclei (IGN) have yielded comparable veloc-

<sup>\*</sup> email: torus@physicist.net

ity profiles, suggesting that the masses of AGN and IGN are similar, if not identical. The vastly differing activity levels could signify an inherent defect with current AGN models. Little theoretical progress seems to have been made over past decades towards a full explanation for these exceedingly energetic phenomena. Closer inspection and revision of existing theories may be necessary to attain a consistent understanding of quasars and AGN. The crucial test of any theory is the correspondence between predictions and observations, it is argued that existing models are struggling in this respect. The purpose of this discussion is to advocate a new model and describe how, with relatively minor theoretical embellishments, compelling explanations for AGN and anisotropic gamma-ray bursts accompanying core-collapse supernovae can be developed. Possible mechanisms responsible for originating, accelerating and collimating jets are then discussed.

The well known black hole uniqueness theorems rest on the classical theory of general relativity. It is thought that any non-distorted and asymptotically flat black hole space-time can be represented by the Kerr-Newman set of solutions. But, while an ultimate theory remains elusive, one cannot be entirely sure of the validity of the uniqueness theorems. Hence, it is important to explore possibilities beyond those anticipated by purely classical calculations. Small departures from classical physics, e.g. of quantum mechanical origin, might lead to profound macroscopic changes, even to the extent that the topology of black hole horizons can be altered. Similarities between a rotating toroidal black hole (TBH) at the galactic centre accreting matter from its surroundings will be compared with observational evidence from quasars, Seyferts, BL Lacertae and blazars, which have long been suspected to be manifestations of the same underlying astrophysical phenomena. Attention will be paid to the formation of such a TBH, its long-term stability in our universe, jet production and its evolution with time. The possibility is examined that quasars may have been present at some stage of almost every galaxy's development in the early universe. A diagram encapsulating the life-cycles of toroidal BHs, in qualitative agreement with those of quasars is finally presented.

## 2 ROTATING TOROIDAL BLACK HOLES AND THEIR FORMATION

It is proposed that the central component of the quasar mechanism is a rapidly rotating black hole with a toroidal event horizon. First, the possible embryonic of formation are addressed. The constituent stars of most observable galaxies are concentrated in the plane of galactic rotation. Direct observations of the cosmic microwave background by the COBE satellite indicates that matter was very evenly distributed throughout the cosmos in earlier times. Thereafter, on the scale of inter-galactic distances, matter must have collapsed under the action of gravity, triggering the emergence of protogalaxies composed of low-density hydrogen and helium gas. Because most galaxies are observed to rotate, these protogalaxies would generally have possessed angular momentum.

Protogalactic gas clouds then draw towards the plane of rotation. Molecules have random velocities but collisions are

relatively infrequent owing to low particle densities. Those with small velocities tend to accumulate at the galactic centre due to net gravitational attraction. However, these particles gain kinetic energy as they proceed towards the centre, preventing the majority from occupying orbits confined to the centremost regions of the galaxy. Instead they tend to cluster in elliptical orbits of larger radii resulting in a relative underabundance of particles at the core, see Fig. 1, curve labelled  $t = 1$ . For a given instant in time, the density within the galactic plane is at a local minimum at the centre, increases with radius to a maximum and thereafter tapers off. As time progresses, the gas distribution becomes more pronounced and collisions between molecules more frequent. The evolution of the distribution in this scenario is qualitatively depicted by the series of gas density curves in Fig. 1. The curve labelled  $t = 4$  represents what may be identified as a toroidal gas cloud. This ultra-low metallicity toroidal proto-star continues to condense as more gas molecules amass until the density and pressure are sufficient for nuclear fusion. The toroidal stars of this model, Fig. 2(a), will exhaust their nuclear fuel exceedingly rapidly as regions suitable for fusion occupy a greater volumetric fraction of toroidal stars than of spheroidal stars.

By comparison with the upper size and mass limits for spheroidal neutron stars, an upper limit can be estimated for the minor radius  $R_2$  of a neutron torus above which collapse to a TBH will result<sup>†</sup>. Simplifying assumptions are employed. First, the density of neutron degenerate material is assumed to remain constant and independent of pressure as for an incompressible fluid. Hydrostatic equilibrium is reached whereby the pressure of the fluid counteracts gravitational compression at all locations. Newtonian approximations will be used to derive the surface gravity. The torus is assumed to have a major radius much larger than the minor radius,  $R_1 \gg R_2$ , so that an infinitely long cylinder approximation is valid. Rotation is neglected. The gravitational field within a sphere of constant density tails off linearly from the surface to the centre, even according to general relativity. It is useful to confirm that gravity within an infinitely long solid cylinder of constant mass density is linearly related to the radial distance from the axis according to a Newtonian analysis.

For points external to spherically symmetric objects, the gravity is known to be equivalent to that of a point particle of equal total mass located at the centre of symmetry, regardless of any radial density variations. Similarly, the external gravity of an infinitely long cylindrically symmetric mass is equivalent to that of a line mass of infinite length located on the axis. To prove this, assign an outer radius to the cylinder of  $R_T$ , a longitudinal coordinate  $x$  along the cylinder's length and angular coordinate  $\vartheta$ . The gravitational field strength at some radius  $a < R_T$  inside the cylinder with longitudinal coordinate  $x = 0$  and angular coordinate  $\vartheta = 0$  is sought. This location is external to a cylinder of radius  $a$  and internal to a cylindrical shell of

<sup>†</sup> At the time of publication, this TBH formation route seemed to me the most likely, avoiding the need for an SBH→TBH transition. Since then, I am of the opinion that the transition can occur in either direction and that the toroidal progenitor is merely an interesting possibility, not an essential ingredient of the model.

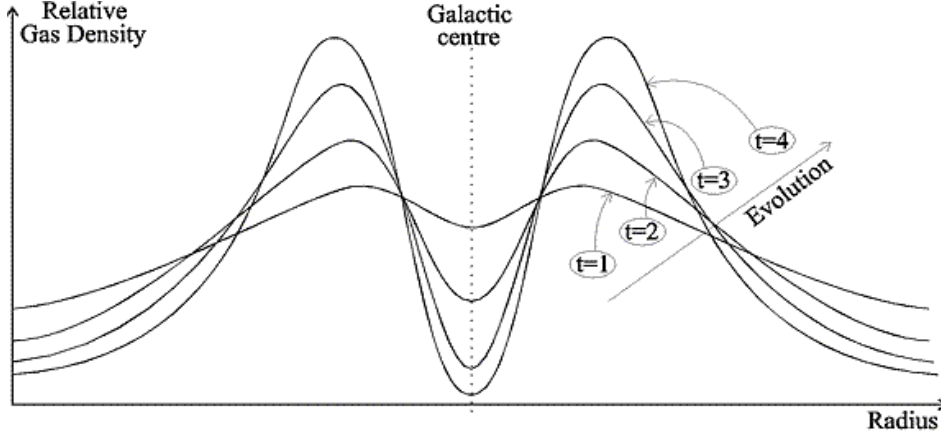


**Figure 1.** Evolution of a rotating, initially collisionless dust cloud. Axial densities decrease with time since these regions can only accommodate particles with both minimum kinetic and gravitational potential energies. Otherwise, the particles are drawn to the equatorial plane and a toroidal structure inevitably develops. Dissipative processes diminish the ellipticity of orbital trajectories.

radial thickness  $b - a$ . Because Newtonian gravity obeys the principle of superposition it is first demonstrated that the gravitational field vanishes at all points located within an infinitesimally thin and infinitely long cylindrical shell with constant mass per unit area  $\sigma$ . Then, by integrating the gravitational contribution of internal cylindrical shells, gravity inside an infinite homogeneous cylinder is observed to vary linearly with radius, as is the familiar variation within homogeneous spheres.

Let the thin cylindrical shell have radius  $b > a$ . Integrating the radially directed gravitational field contributions of elemental masses of constant radius  $b$  over the integration variables  $x$  and  $\vartheta$ , an expression is obtained of the form:

$$g(a) = 2G\sigma \int_0^\pi \int_{-\infty}^{+\infty} \frac{b(a - b \cos \vartheta)}{(a^2 + b^2 - 2ab \cos \vartheta + x^2)^{3/2}} dx d\vartheta \quad (1)$$

Integrating with respect to  $x$  gives:

$$g(a) = 2G\sigma \left[ \frac{x}{\sqrt{x^2 + a^2 - 2ab \cos \vartheta + b^2}} \right]_{-\infty}^{+\infty} \times \int_0^\pi \left( \frac{ab - b^2 \cos \vartheta}{a^2 - 2ab \cos \vartheta + b^2} \right) d\vartheta$$

thus, 
$$g(a) = 4G\sigma \int_0^\pi \frac{ab - b^2 \cos \vartheta}{a^2 - 2ab \cos \vartheta + b^2} d\vartheta \quad (2)$$

Splitting the integral in two, integrating with respect to  $\vartheta$  and recalling that  $b > a$  yields:

$$g(a) = 4\pi G\sigma ab \left( \frac{1}{|b^2 - a^2|} - \frac{1}{b^2 - a^2} \right) = 0 \quad (3)$$

It is therefore possible to ignore the gravitational contribution of cylindrical shells with radii larger than  $a$  and consider only the internal cylinder of radius  $a$ . When the previous integral is recalculated for the case where  $a > b$  it is found that:

$$g(a) = \frac{4\pi G\sigma b}{a} \quad (4)$$

To transform to a volumetric calculation,  $\sigma$  is replaced by a three-dimensional mass density  $\rho$  and  $g$  is summed over cylindrical shells from  $b = 0$  to  $b = R_T$  to find the surface

gravity of a torus in an infinite cylinder approximation:

$$g_T = \int_0^{R_T} \frac{4\pi G\rho b}{R_T} db = 2\pi G\rho R_T \quad (5)$$

which also shows that the gravity within an infinite cylinder varies linearly with radius. Mass density  $\rho$  is assigned to both the toroidal and spherical neutron stars. The radius of the neutron sphere is  $R_S$  and the minor radius of the neutron torus  $R_T$ . For a sphere, surface gravity  $g_S$  can be immediately calculated:

$$g_S = \frac{GM_{\text{sphere}}}{R_S^2} = \frac{4\pi G\rho R_S}{3} \quad (6)$$

By calculating the pressure at the centre of the sphere ( $P_{SC}$ ) and torus ( $P_{TC}$ ), then equating the two values, it will be possible to compare the limiting radii at which further gravitational collapse takes place. The surface pressures are assumed to be zero and integration is performed over infinitesimally thin (spherical or cylindrical) shells of matter. The pressure difference between the inner and outer surface of a shell is given by the weight of the shell divided by the area of the inner shell surface. Noting that the weight of the shell depends on the local value of gravity, which is constant throughout the shell and a linear function of radius from zero at the centre to  $g_S$  or  $g_T$  at the surface, one can write:

$$P_{SC} = \frac{\rho g_S}{R_S} \int_0^{R_S} r dr = \frac{\rho g_S R_S}{2} = \frac{2\pi G\rho^2 R_S^2}{3} \quad (7)$$

$$P_{TC} = \frac{\rho g_T}{R_T} \int_0^{R_T} r dr = \frac{\rho g_T R_T}{2} = \pi G\rho^2 R_T^2 \quad (8)$$

Equating  $P_{SC}$  and  $P_{TC}$  allows the determination of an upper limit for the minor radius of a neutron torus in terms of the maximum neutron sphere radius. Note that this result is independent of the density of neutron star matter and that the reliability of the result is improved by the balancing of the Newtonian approximations:

$$R_{T_{\text{max}}} = \sqrt{\frac{2}{3}} \times R_{S_{\text{max}}} \approx 8.5 \text{ km} \quad (9)$$

As might be expected, the minor radius of an infinitely long neutron cylinder must be smaller than the maximum spherical radius. In circumstances where the infinite cylinder

approximation is invalid, the minor radius will be further constrained. If general relativity were to be used then the pressure gradient for a spherical star would be given by the standard equation describing hydrostatic equilibrium:

$$\frac{dP}{dr} = -G \frac{(\rho + P/c^2)[m(r) + 4\pi r^3 P/c^2]}{r[r - 2Gm(r)/c^2]} \quad (10)$$

Here  $P$  is the pressure at some radius  $r$  and  $m(r)$  is the mass enclosed by the 2-sphere defined by  $r$ , whose internal density may vary with radius according to a chosen equation of state. General relativity requires larger neutron degeneracy pressures if gravity is to be resisted, but the estimate of (9) is adequate for the present discussion.

Confining the discussion to those toroidal stars whose gravitational implosion directly results in a TBH rather than intermediate white dwarf or neutron density phases, the pre-collapse seed star is assumed to be incompressible and of solar density  $\sim 1400 \text{ kg m}^{-3}$ . For the purposes of approximation, the surface areas of extremal Kerr BH event horizons are equated with the surface areas of TBHs with equal mass, alternatively this may be viewed as equating the entropy of the BHs. The TBH is assumed to have an angular momentum equal to the extremal Kerr BH of equal mass. In addition, the TBH geometry will be taken to be that of an Euclidean torus parameterised by the major and minor radii  $R_1$  and  $R_2$  respectively. This crude model permits the preparation of order of magnitude estimates.

An extremally rotating Kerr BH has  $r_+ = m$  so its area is  $A = 4\pi r_+^2 = 4\pi m^2$ . The surface area of an Euclidean torus is  $A = 4\pi^2 R_1 R_2$  so, to a good approximation, the rotating TBH mass is related to the TBH area by equating these two expressions for area and, after restoring the natural constants ( $r_+ = Gm/c^2$ ), it is found:

$$M_{\text{TBH}} \approx \frac{c^2}{G} \sqrt{\pi R_1 R_2} \quad (11)$$

Now consider a (low density) toroidal star (TS) of Euclidean geometry whose major radius is  $R_1$  as before, but with a minor radius  $R_3$ . Evidently  $R_3 > R_2$  otherwise the TS is a TBH and  $R_3 < R_1$  ensures the star is toroidal. The TS undergoes gravitational collapse once its nuclear fuel is exhausted and the resulting TBH is assumed to have the same major radius  $R_1$  as the TS. Since the volume of the TS is  $V_{\text{TS}} = 2\pi R_1 R_3^2$ , and the TS is composed of constant density material  $\rho \sim 1400 \text{ kg m}^{-3}$  then the mass of the toroidal star will be  $M_{\text{TS}} = 2\pi \rho R_1 R_3^2$ . Following a supernova (SN) implosion of the star, typically most of the mass will have been ejected. A parameter  $\eta$  represents the fraction of the original TS mass remaining in the TBH after the SN. The remaining mass is identified with the mass of the resultant TBH so that:

$$\frac{c^2}{G} \sqrt{\frac{R_2}{4\pi R_1}} \approx \rho \eta R_3^2 \quad (12)$$

Having already determined the maximum minor radius of a neutron torus in (9) this implies:

$$R_1 > R_2 \gtrsim 8.5 \text{ km} \quad (13)$$

Taking the limit as  $R_3 \rightarrow R_1$  with  $R_3 < R_1$  in (11) and using the relation  $M_{\text{TBH}} = \eta M_{\text{TS}}$  with  $\eta = 0.1$  (90% mass ejection) gives a limit for TBH formation:

$$\frac{R_1^5}{R_2} > \frac{c^4}{4\pi \rho^2 \eta^2 G^2} \approx 7.4 \times 10^{48} \text{ m}^4 \quad (14)$$

Allowing  $R_2 \rightarrow 8.5 \text{ km}$  with this condition gives a lower bound for  $R_1$ :

$$R_1 \gtrsim 36 \times 10^9 \text{ m} \quad (15)$$

If the TS grows too large and too massive, then it will become a TBH without an implosion or electron/neutron degeneracy supported phases. Since the area of the TS is larger than the area of a TBH of the same mass, then  $R_3 > R_2$  because  $R_1$  is common to both. Consideration of (12) in the case where  $R_3 \rightarrow R_2$  then leads to:

$$R_1 R_2^3 < \frac{c^4}{4\pi \rho^2 \eta^2 G^2} \approx 7.4 \times 10^{48} \text{ m}^4 \quad (16)$$

The SN is assumed to shed 90% of the original star's mass during the implosion (this assumption is the least reliable and easily dominates the combined errors of the remaining assumptions). In special cases where  $R_2$  approaches  $R_1$  and the inequalities hold then almost no mass is lost because the star does not collapse much before the event horizon engulfs it. Since it has been assumed that the major radius is unchanged during collapse, conservation of angular momentum dictates that the angular velocity of the resulting BH will match that of the seed star. Hence, less mass ejection is anticipated than in more familiar SN events wherein a star collapses to form a spheroidal BH with very high angular velocity. For a given  $R_2/R_1$  ratio, the permissible range of toroidal star masses which can gravitationally collapse to form a TBH range is typically quite broad (Fig. 9). This issue is returned to later.

These massive toroidal stars would have rapidly exhausted their nuclear fuel. Regions suitable for fusion reactions occupy a much larger proportion of the total stellar volume in toroidal stars than in spherical stars. The end result would be a supernova-like implosion, most likely the first SN event of its host galaxy, presumably localised to one portion of the torus initially, Fig. 2(b). Because the implosion is limited by the speed of light, it could take several hours for the implosion to propagate around the torus in both directions, Fig. 2(c), until the implosion fronts meet at the opposite end of the torus. During the implosion a thin tubular event horizon expands along the torus, eventually encountering itself and sealing to provide a stable TBH, Fig. 2(d). The illustrations of Fig. 2 are not based upon precise physical calculations, they are merely intended show the progression of the gravitational implosion around the torus.

The mass of the toroidal star is such that if as much as 90% of its mass is outwardly expelled during the SN implosion, there will still remain enough mass to construct what must inevitably become a BH rather than a neutron star remnant. Suppose that much more of the mass is ejected during the SN, perhaps 99%, then what may remain could conceivably be a toroidal white dwarf or toroidal neutron star. In either case, turbulence and dissipative processes are unlikely to leave these delicate structures unchanged. If macroscopic axisymmetry is retained, e.g. through electromagnetic confinement of the torus, then after a brief period the torus will evolve to a smaller major radius. As this occurs, an increase in either its minor radius, its density or, more likely both ensues. Therefore, toroidal white dwarves could become toroidal neutron stars and toroidal neutron stars could become toroidal black holes. Toroidal neutron stars of masses  $\sim 10^6 M_\odot$  are precluded as serious AGN

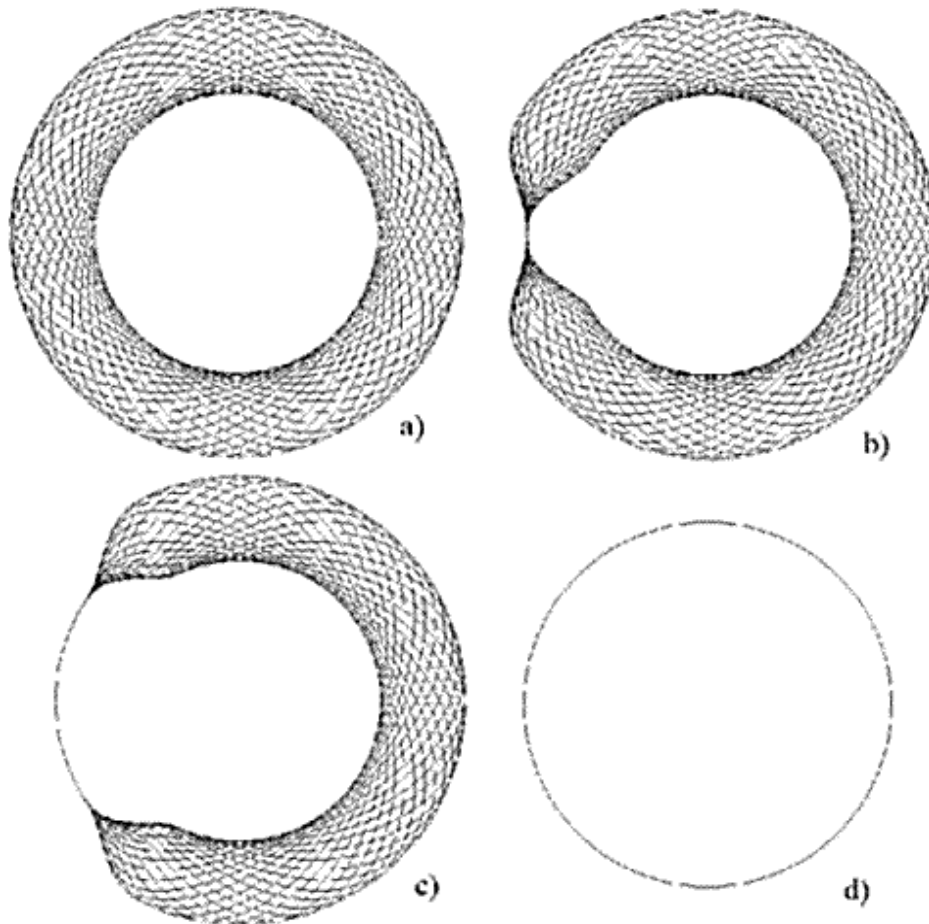


**Figure 2.** Gravitational collapse of a toroidal star to a TBH. Collapse initially localised to one region of the torus (b) propagates bi-directionally around the torus until implosion fronts meet and the TBH topology is established.

candidates by their limited lifespan, slender geometry and inability to endure sustained accretion. Smith and Mann (1997) have recently investigated gravitational collapse as a TBH formation mechanism starting with collisionless particles of random velocities but zero net angular momentum.

Quasar observations yield spectra with very strong metallic absorption lines. The population II stars of the galactic centre would mainly consist of Hydrogen and Helium, which has previously troubled spheroidal BH quasar models. Because SNe are efficient at generating heavy elements, the TBH creation SN would have scattered a substantial amount of metallic elements into the ambient galactic environment, imparting its signature on the radiation spectrum of the central engine.

### 3 STABILITY OF ROTATING TOROIDAL BLACK HOLES

For some time, following the work of Hawking (1972) and Hawking & Ellis (1973), it was thought that TBHs were unstable, albeit marginally. This somewhat contra-intuitive result assumed that Einstein's cosmological constant ( $\Lambda$ ) was zero. Numerical computations of collisionless particles resulting in a transient toroidal event horizon (terminating in a sub-extremal Kerr BH) and assuming  $\Lambda = 0$  were performed

by Abrahams et al (1994), Hughes et al (1994) and Shapiro, Teukolsky & Winicour (1995). These results were consistent with the topological censorship theorem of Friedman, Schleich & Witt (1993) which implies that a light ray cannot pass through the central toroidal aperture before the topology becomes spherical. More recently, papers by Huang & Liang (1995), Aminneborg et al (1996), Mann (1997), Vanzo (1997) and Brill (1997) have provided mathematical descriptions of TBHs within the framework of general relativity. These equations assume that the cosmological constant is negatively valued to admit stability for the TBH and is literally constant throughout the spacetime described, which has an anti-de Sitter (AdS) background. The Vanzo paper claims that a TBH can exist in a virtually flat spacetime because the TBH size is determined by the mass and conformal class of the torus, not by the cosmological constant. Rotating charged black (cosmic) strings have been described by Lemos & Zanchin (1996). A spacetime metric for a rotating, uncharged TBH presented by Klemm, Moretti & Vanzo (1998), is hereafter referred to as the KMV metric. This metric is not unique, but it is the first generalisation to admit rotation of TBHs. Holst & Peldan (1997) showed that rotating Banados-Teitelboim-Zanelli (BTZ) BHs cannot be described in terms of a 3+1 split of spacetime, instead spacetimes of non-constant curvature are required.

Physical measurements to date have been unable to establish conclusively whether  $\Lambda$  is positive or negative. The accelerating cosmological recession of distant SNe favours a positive value, though whether this recession is attributable to a cosmological constant is the subject of continuing debate. Arguments against TBH stability have assumed that in our universe, the constant is precisely zero everywhere. The weak energy condition is assumed to be satisfied, although it is known to be violated in certain situations e.g. Casimir effect and Hawking radiation. Topological BHs in anti de-Sitter spacetimes are now known not to conflict with the Principle of Topological censorship, for a recent discussion, see Galloway et al (1999). Intuitively, rotating TBHs are not dissimilar to Kerr BHs in that both contain ring singularities whose radii are determined by the angular momentum assuming constant BH mass. One extra parameter is necessary to characterise a stationary TBH in addition to the mass, angular momentum and charge of the Kerr-Newman metric. This parameter determines the exact geometry of the torus and can be expressed as the ratio of the minor and major radii  $R_2/R_1$  (as used here) or the ratio akin to a Teichmüller parameter presented by the KMV paper. Stationarity is preserved only when this parameter achieves a balance with the TBH mass and angular momentum, and to a lesser degree the charge.

It was demonstrated by Gannon (1976) that for non-stationary BHs in asymptotically flat spacetimes, the topology of the event horizon must be either spherical or toroidal. A rotating TBH located at the centre of a galaxy surrounded by accreting matter is manifestly non-stationary. The stationary BH metrics containing physical singularities are acutely idealised, the Kerr metric contains a ring singularity surrounded by vacuum i.e. a universe devoid of other matter. This is a gross simplification of what would be found in nature. Inside the inner event horizon  $r_-$ , particles are not compelled to collapse towards the singularity, but are free to explore all radii  $0 \leq r \leq r_-$ . Suppose a Kerr BH forms by the collapse of a non-rotating neutron star. The matter at the surface of the neutron star can reach the singularity in a finite proper time. On the other hand, viewed from infinity, this matter never crosses the event horizon, less still reaches the singularity. According to distant observers, the matter is frozen fractionally above the event horizon. Just as infalling matter experiences the crossing of outer then inner event horizons in finite time, it also witnesses the end of the external universe before nearing the singularity. The only possible answer to the question: “when does the BH become stationary to distant observers?” is never. Indeed, one might venture that truly stationary spacetimes are forbidden. It is dangerous to be guided by predictions about BH stability which rely on stationarity as one of the underlying assumptions.

Perhaps there is some deeper significance underlying the unobtainability of stationarity. Consider a closed universe approaching a big crunch and contracting rapidly in all directions. The surface defining the outer reaches of this universe could be considered as the event horizon of a BH beyond which spacetime does not exist in the usual sense. This is a BH that could conceivably approach stationarity in a short and finite time as measured by the clocks of all internal observers, there being no external observers. A singularity develops which is accessible to all the infalling mat-

ter. The outermost layers of the imploding universe catch up with the innermost layers at the Cauchy horizon, the surface of infinite blue shift. A vacuum develops in the region surrounding the singularity as it swiftly becomes devoid of matter and stationarity is achieved. The singularity now contains the entire mass of the pre-collapse universe and the Pauli exclusion principle does not participate in the physics of the singularity. What grounds are there for discarding the Pauli exclusion principle? This principle has successfully predicted the existence of white dwarfs and neutron stars. Could quark degeneracy arise? What might string theory predict? There are obvious similarities between the Pauli exclusion principle and the premise that stationary BHs are forbidden. If it is true that BHs truly abhor stationarity then presumably re-expansion would be the only option.

Suppose that a TBH with a substantial central aperture is rotating in asymptotically flat space with a near maximal angular momentum (event horizon velocity approaching the speed of light). In principle, there is no reason why the rotational energy of this TBH cannot be arbitrarily larger than the TBH’s rest mass, whereas a Kerr BH can only hold at most 29% of its total energy in rotational form, the remainder being the irreducible mass. According to topological censorship, the TBH must become spheroidal before a light ray can traverse the aperture. The fate of the excess rotational energy is something of a conundrum. Is the excess energy hastily expelled by some undiscovered mechanism? Is topological censorship flawed? Would the TBH break up into multiple co-rotating spheroidal BHs? Does the Kerr BH rotate above the extremal limit, and if so is the singularity revealed? These problems can be circumvented for now by assuming a negative  $\Lambda$ .

It seems somewhat coincidental that the cosmological constant is so nearly zero and not very much larger in value, on purely theoretical grounds a value 120 orders of magnitude greater than observational limits might have been expected. One plausible suggestion was proposed by Coleman (1988). According to the author, macroscopic cancellation mechanisms operate on the zero point energies under normal circumstances and these result in a zero expectation for  $\Lambda$ . The situation is, however, complicated in the presence of intense gravitational fields generated by BHs, particularly in the immediate vicinity of the singularities residing within the event horizons. Under such conditions, the cancellation of zero point energies operates imperfectly and gives rise to what may be considered a localised but substantial cosmological ‘constant’. By this means, TBH stability could be ensured within a universe where elsewhere  $\Lambda$  is small. It was also suspected that zero point energy might play a part in the physics of curved spacetimes because of imperfect cancellations complicating the assumptions underlying the quantum mechanical technique of renormalization (Misner, Thorne & Wheeler 1973). It comes as little surprise that quantum effects may play a prominent role when the spacetime of classical general relativity becomes singular, the stability of the TBH structure could prove to be the only direct evidence of this.

The KMV metric has axial symmetry and the horizons are Riemannian surfaces of constant gravity that obey the familiar BH entropy-area laws. Utilising the membrane paradigm approach (Thorne, Price & MacDonald 1986) simplifies the consideration of the physics of these BHs out-

side the event horizon. The fact that these objects are thermodynamically well behaved, whilst interesting, is of little relevance to the present discussion. Parallels between rotating TBH solutions and the Kerr solutions for spinning spheroidal BHs may be drawn, for instance both have ergoregions external to their event horizons and the maximum angular momentum of each is bounded for a given mass. Conservation of mass and angular momentum is known to be satisfied. A maximally rotating Kerr BH has a static limit extending to  $2m$ , double the radius of the outer event horizon. The equator of the static limit surface circles with the speed of light at extremality. The ergoregion occupies the region between the static limit and the event horizon within which everything is compelled to co-rotate with the BH due to the spacelike character of the time coordinate. Similarly, the maximal KMV metric determines the ratio  $r_s/r_+$  to be 1.59. Orbits within 300% of the extremal Kerr event horizon radius are unstable and matter (the accretion disk) tends to be drawn towards the BH. For a maximally rotating BH, entering the ergoregion becomes impossible because incoming particles would have to travel ‘faster’ than light and possess an infinite amount of energy. Similarly, if the BH is rotating slightly below this rate then only a tiny fraction of the external particles will penetrate the ergoregion, those with very high kinetic energies.

An ergoregion enshrouds the toroidal event horizon of the KMV metric. Fig. 3 depicts a cross-sectional view of a rotating TBH. The event horizon will be enshrouded by an ergoregion which, depending upon the precise geometry of the TBH, might entirely seal the central aperture. Beyond the ergoregion lies what is sometimes referred to as a zone of unstable orbits within which particles are unable to establish repeating orbital patterns by following geodesic pathways. The ergoregion does not intersect the event horizon at any point, as it does at the poles of a Kerr BH. Particles cannot penetrate the ergoregion of a maximally rotating TBH, whichever trajectory is attempted. The maximal rotation rate will not be achieved in practice because the BH is able to reduce its rotation rate by several methods which are relevant to jet formation and several theoretical reasons such as the fact that the internal singularity would become naked, even as viewed from infinity.

#### 4 METRIC OF ROTATING TOROIDAL BLACK HOLE

The KMV metric of an uncharged rotating TBH in asymptotically anti de-Sitter (AdS) spacetime is tentatively forwarded as a model for the naturally occurring TBH. The primary reservations concerning the physical applicability of the topological BH metrics in AdS gravity are that  $\Lambda$  is assumed to be independent of location and, contrary to the most reliable observations, negative in value. Given the uncertainty regarding the role of quantum mechanics in BH physics, these assumptions may be invalid. The metric describes a vacuum solution of Einstein’s equation which has reached equilibrium after an infinite coordinate time has elapsed. It possesses a ring singularity, but no provision for accreting matter has been made. Indeed, a massive accretion disk may act as a stabilising influence on a TBH within an asymptotically flat spacetime (further discussed in ap-

pendix B). A negative cosmological constant may be thought of as contributing a cosmological attraction. In its absence, the combination of a host galaxy’s matter and the nearby massive accretion disk surrounding the outer periphery of a TBH located within a galactic nucleus may provide a natural substitute for the stabilising negative  $\Lambda$  used in the AdS metrics.

With these considerations in mind, attention is focused on the KMV metric which, for convenience, is now recalled:

$$ds^2 = -N^2 dt^2 + \frac{\rho^2}{\Delta_r} dr^2 + \frac{\rho^2}{\Delta_P} dP^2 + \frac{\Sigma^2}{\rho^2} (d\phi - \omega dt)^2 \quad (17)$$

where the following relations apply:

$$\rho^2 = r^2 + a^2 P^2 \quad (18)$$

$$\Sigma^2 = r^4 \Delta_P - a^2 P^4 \Delta_r \quad (19)$$

$$\Delta_r = a^2 - 2mr + r^4/l^2 \quad (20)$$

$$\Delta_P = 1 + \frac{a^2 P^4}{l^2} \quad (21)$$

$$N^2 = \frac{\rho^2 \Delta_P \Delta_r}{\Sigma^2} \quad (22)$$

$$\omega = \frac{\Delta_r P^2 + r^2 \Delta_P}{\Sigma^2} a \quad (23)$$

Here, the angular velocity is  $\omega$ , the equatorial angle is  $\phi$ ,  $P$  is another angular variable with some period  $T$ ,  $r$  is a pseudo-radial coordinate,  $a$  is the angular momentum per unit mass and  $l$  is defined as  $\sqrt{-3/\Lambda}$ . The ratio of  $T$  to  $2\pi$  is analogous to the Teichmüller parameter describing a flat torus in Riemannian geometry. TBH mass by the ADM definition is  $M = mT/2\pi$  and angular momentum  $J = Ma$ . The coordinate  $r$ , as in the Boyer-Lindquist form of the Kerr metric, is only a true radial coordinate as  $r \rightarrow \infty$  with  $r = 0$  the location of a ring singularity not corresponding to zero radius. Unlike the Kerr BH, as  $r \rightarrow -\infty$  within the equatorial plane, this point is outside the event horizon. It would be preferable to introduce a coordinate transformation whereby  $r' = f(r)$  such that  $f(\infty) = \infty$ ,  $f(0) = a$  (say) and  $f(-\infty) = 0$  and select  $f(r)$  such that  $r'$  is an affine parameter, but this is beyond the scope of the present discussion.

In order for the metric to describe a torus,  $P$  is a periodic variable with period  $T$  and is covered by four patches  $P = \lambda \sin \vartheta$  at  $\vartheta = 0$  and  $\vartheta = \pi$ , and  $P = \lambda \cos \vartheta$  at  $\vartheta = \pi/2$  and  $\vartheta = 3\pi/2$  where  $\lambda$  is a constant such that  $T = 2\pi\lambda$ . Between these points the behaviour is defined by  $\cos \vartheta$  being some  $C^\infty$  function (infinitely differentiable) of  $\sin \vartheta$  and vice versa.

Upon inspection of the metric, (17), it can be seen that  $\Delta_r$  in (20) becomes zero at the event horizon. Inner and outer event horizons exist as real and positive roots of the quartic equation with real coefficients:  $r^4 - 2ml^2 r + a^2 l^2 = 0$  along with two other physically less meaningful complex conjugate roots. For the extremally rotating case,  $a = a_c = \sqrt{3} \times \sqrt[3]{lm^2/4}$  and these two roots coincide. It is straightforward to verify that the real roots are  $r_{\pm} = \sqrt[3]{ml^2/2}$ .

The ergoregion is defined as the region between the outer event horizon and the static limit hypersurface at which the metric coefficient of  $dt^2$  vanishes altogether, i.e.  $g^{tt} = \omega^2 \Sigma^2 / \rho^2 - N^2$  which is solved for  $r$  by another quartic  $r^4 - 2ml^2 r - a^4 P^4 = 0$ . This polynomial has one real

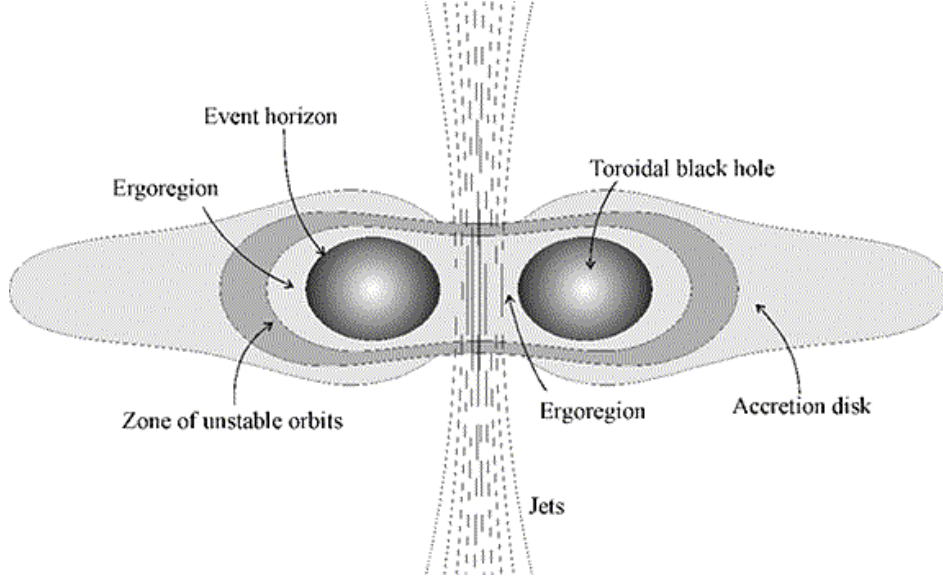


**Figure 3.** Meridional section of a rotating TBH producing jets when matter accretes from a surrounding disk illustrating the approximate form of the ergoregion and limiting boundary for stable orbits.

and positive root, one real and negative root and two complex conjugate roots. The real positive root has a minimum value of  $\sqrt[3]{ml^2}$  for  $P = 0$  which is larger than  $r_+$  by a factor of 1.59. The static limit hypersurface is well separated from the event horizon and, unlike the poles of the Kerr situation, these surfaces are nowhere contiguous. Therefore, a substantial ergoregion is observed.

Examining the equatorial plane by setting  $dP = P = 0$  the metric reduces to:

$$ds^2 = -\left(\frac{r^2}{l^2} - \frac{2m}{r}\right) dt^2 + \left(\frac{r^2}{l^2} - \frac{2m}{r} + \frac{a^2}{r^2}\right)^{-1} dr^2 \quad (24)$$

In order to determine the trajectories of null geodesics within this hypersurface use can be made of the Euler-Lagrange equations with  $K = ds^2/2$ :

$$\frac{\partial K}{\partial x^a} - \frac{d}{du} \left( \frac{\partial K}{\partial \dot{x}^a} \right) = 0 \quad (25)$$

the overdot denoting differentiation with respect to some affine parameter  $u$ . The equatorial metric (24) may be partial differentiated with respect to  $t$  and  $\phi$  respectively then integrated with respect to  $u$  to give:

$$\left(\frac{2m}{r} - \frac{r^2}{l^2}\right) t - a\dot{\phi} = \alpha \quad (26)$$

$$r^2\dot{\phi} - at = \beta \quad (27)$$

Where  $\alpha$  and  $\beta$  are constants of integration. A third constant  $\gamma = \alpha/\beta$  can be defined and used to relate both equations:

$$\left(\frac{2m}{r} - \frac{r^2}{l^2}\right) t - a\dot{\phi} = \gamma(r^2\dot{\phi} - at) \quad (28)$$

which upon rearrangement reads:

$$\frac{d\phi}{dt} = \frac{\dot{\phi}}{t} = \frac{2ml^2 - r^3 + \gamma arl^2}{arl^2 + \gamma l^2 r^3} \quad (29)$$

Next, boundary conditions are imposed by considering the extremal case  $a = a_c$  for which the angular velocity at

the event horizon  $r_+$  is, using the expressions for  $a_c$  and  $r_+$  and noting that  $\omega = a/r^2$  in the equatorial plane.

$$\left. \frac{d\phi}{dt} \right|_{r=r_+} = \Omega_H = \frac{a_c}{r_+^2} = \frac{\sqrt{3}}{l} = \frac{2ml^2 - r_+^3 + \gamma ar_+ l^2}{ar_+ l^2 + \gamma l^2 r_+^3} \quad (30)$$

Some algebra reveals that the constant of proportionality  $\gamma$  obeys the relations:

$$\gamma = \frac{3\sqrt[3]{2}ml - 2\sqrt{3}a\sqrt[3]{ml^2}}{\sqrt{3}\sqrt[3]{2}ml^2 + 2al\sqrt[3]{ml^2}} = \frac{3r_+^2 - \sqrt{3}al}{\sqrt{3}lr_+^2 + al^2} \quad (31)$$

So now the rate of change of  $\phi$  with respect to coordinate time  $t$  is fully determined. Following straight from the metric and the condition that  $ds = 0$  for null geodesics:

$$\left(\frac{2m}{r} - \frac{r^2}{l^2}\right) \dot{t}^2 + \left(\frac{r^2}{l^2} - \frac{2m}{r} + \frac{a^2}{r^2}\right)^{-1} \dot{r}^2 + r^2 \dot{\phi}^2 - 2a\dot{\phi}\dot{t} = 0 \quad (32)$$

Dividing throughout by  $(dt/du)^2$  eliminates the affine variable allowing  $dr/dt$  to be found using the previously derived expression for  $d\phi/dt$ :

$$\frac{dr}{dt} = \sqrt{\left[2a\frac{d\phi}{dt} - r^2\frac{d\phi^2}{dt} + \frac{r^2}{l^2} - \frac{2m}{r}\right] \left[\frac{r^2}{l^2} - \frac{2m}{r} - \frac{a^2}{r^2}\right]} \quad (33)$$

It would be possible to continue this analysis by integrating with respect to  $t$  for each variable  $r$  and  $\phi$ , resulting in cumbersome mathematical terms. It is sufficient for now to say that these equations allow the null congruences of the equatorial plane to be readily determined by numerical methods.

## 5 ROTATING TOROIDAL BLACK HOLE IN ASYMPTOTICALLY FLAT SPACE

In order to visualise a TBH in asymptotically flat space and its effect on local spacetime, a method which approximates the time dilation at locations in space surrounding arbitrarily complex mass configurations is now introduced. First,

the time dilation is derived for the Schwarzschild spacetime with metric:

$$ds^2 = \left(1 - \frac{2m}{r}\right) dt^2 - \left(1 - \frac{2m}{r}\right)^{-1} dr^2 - r^2 (d\vartheta^2 + \sin^2\vartheta d\phi^2) \quad (34)$$

The event horizon of this static spacetime occurs when  $g^{rr}$  becomes infinite, or  $r_+ = 2m$  in geometrical units. Consider the time dilation of a stationary particle located at some constant  $r$ ,  $\vartheta$  and  $\phi$ . The metric interval  $ds$  can be interpreted as the proper time of particles travelling on time-like paths so that  $d\tau = ds$ . The time dilation may be read from the metric at once as:

$$\frac{d\tau}{dt} = \sqrt{\left(1 - \frac{2m}{r}\right)} = \sqrt{\left(1 - \frac{r_+}{r}\right)} = \sqrt{\psi} \quad (35)$$

$$\text{where } \psi = \left(1 - \frac{2m}{r}\right) \quad (36)$$

As  $r \rightarrow \infty$  notice that  $d\tau/dt = 1$  whilst  $d\tau/dt$  decreases towards zero as the event horizon is approached, as expected. Now, the particle is allowed to undergo radial motion  $dr \neq 0$ ,  $d\vartheta = d\phi = 0$ . The metric is divided throughout by  $dt^2$  and the particle's radial velocity in local coordinates is given by  $v_p = dr/d\tau$ . This yields a similar equation to the last but with the introduction of a  $v_p$  dependent term:

$$\frac{d\tau}{dt} = \frac{\psi}{\sqrt{\psi + v_p^2}} \quad (37)$$

For the Schwarzschild BH, the event horizon and stationary limit coincide at  $r = r_+$  and  $d\tau/dt$  becomes zero there. A radial velocity can affect the time dilation but cannot alter the location of the hypersurface at which the time dilation approaches zero. Conversely, in the Kerr case which is now briefly addressed,  $d\tau/dt$  becomes zero for stationary particles outside the event horizon on the stationary limit, the outermost boundary of the ergosphere. Particles motionless with respect to distant observers will appear to freeze at the static limit but particles in prograde orbits can both penetrate and escape the ergosphere in a finite coordinate time. For retrograde orbits, the time dilation approaches zero at radii beyond the static limit so the location of the stationary limit is meaningful only for particles with zero coordinate velocity. The ergosphere is a zone where some particles are able to travel on spacelike trajectories — these trajectories becoming increasingly probable close to the outer event horizon. Whereas negative energy states are only available within the ergosphere of a Kerr BH, a charged Kerr-Newman BH offers negative energy states beyond the static limit.

Returning to the Schwarzschild metric, situations where the particle undergoes transverse (azimuthal) motion are examined by setting  $dr = 0$  and  $d\vartheta = 0$ . Noting that  $v_p = r^2 d\phi/d\tau$  this leads to:

$$\frac{d\tau}{dt} = \sqrt{\frac{\psi}{1 + v_p^2}} \quad (38)$$

The next task in this analysis is to derive approximations for the time dilation experienced by observers nearby a moving point mass where the clock at infinity is motionless relative to the nearby observers. This cannot be read directly from the Schwarzschild coordinates since the mass of the singularity is stationary with respect to observers at infinity. By taking the limit as  $m \rightarrow 0$  one obtains  $\psi \rightarrow 1$

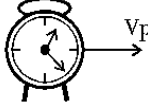
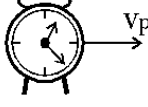
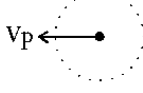
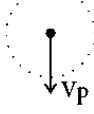
and both the previous equations reduce to the time dilation of special relativity when two objects are in relative motion. These limits are used to introduce a contribution to the time dilation equivalent to inducing a motion of the clocks at infinity. The situation then describes clocks at infinity moving with velocity  $v_p$ , clocks of local observers moving with velocity  $v_p$  and a motionless point mass. Since all inertial frames are equivalent, one can think of this as stationary clocks and a moving mass with velocity  $v_p$  in the opposite direction. The various possibilities are depicted in Fig. 4. Condition 6 has been determined by taking the ratio of the expression in condition 4 with the expression in condition 2. Likewise, condition 7 has been determined by taking the ratio of the expression in condition 5 with the expression in condition 3. By taking these ratios, Lorentzian boosts are applied which remove the time dilation contributions of expressions 4 and 5 which were purely due to the relative motions of the clocks. What remains are motionless clocks in the presence of a moving point mass.

The expressions in conditions 2 and 3 are identical implying that time dilation between observers in the absence of gravity is independent of the direction of motion. Conditions 2 and 3 are limiting cases of conditions 4 and 5 respectively in the absence of matter. The parity between the expressions of conditions 1 and 7 suggests that only the component of the mass's velocity towards the local clock (not the clock at  $\infty$  since this is always unaffected by the mass) contributes to the time dilation of the local clock relative to the clock at infinity. Condition 6 can then be used to calculate the time dilation precisely in more general circumstances providing that  $v_p$  is the velocity component towards the local clock. Note also that there is no requirement for the clocks and the mass to be aligned as they are in Fig. 4, the expressions presented are valid for all configurations owing to the perfect spherical symmetry of the Schwarzschild geometry.

Suppose the Schwarzschild point singularity is subdivided into  $N$  smaller but not necessarily equal masses, each point mass being located at  $r = 0$ , the same spatial position as the parent singularity. In order to accurately recover the time dilation of (35), one is obliged to perform  $N$  summations of the ratios  $r_+/r$  where  $r_+$  relates to the Schwarzschild radius of the mass of each child singularity in turn according to the equation  $r_+ = 2m_{\text{child}}$ . This will be generalised for the purposes of approximation such that the point masses are not coincident but are located separately in space. Thus the distance  $r$  will in general be different for each point mass. Restoring natural constants, the following equation is obtained:

$$\frac{d\tau}{dt} = \sqrt{1 - \frac{2G}{c^2} \times \sum_n \frac{M_n}{R_n}} \quad (39)$$

This may be thought of as a pseudo-principle of superposition and these results may be used to approximate an asymptotically flat spacetime containing a ring singularity. Firstly, the discussion is confined to a momentarily stationary ring singularity i.e. one with zero angular velocity and a radius  $R_1$  whose derivative with respect to time is momentarily zero. An expression for the time dilation relative to observers at infinity experienced by a spatially fixed observer due to the momentarily motionless ring singularity is derived. The singularity is assigned a constant mass per unit length  $b$  and radius  $a$  such that the total mass is  $2\pi ab$ . The

Condition	Clock at $\infty$	Local clock	Point mass	Time dilation
1. Mass and clocks stationary				$\frac{d\tau}{dt} = \sqrt{\Psi}$
2. Local clock undergoing radial motion with mass $m=0, \Psi=1$				$\frac{d\tau}{dt} = \frac{1}{\sqrt{1+V_p^2}}$
3. Local clock undergoing transverse motion with mass $m=0, \Psi=1$				$\frac{d\tau}{dt} = \frac{1}{\sqrt{1+V_p^2}}$
4. Local clock undergoing radial motion				$\frac{d\tau}{dt} = \frac{\Psi}{\sqrt{\Psi+V_p^2}}$
5. Local clock undergoing transverse motion				$\frac{d\tau}{dt} = \frac{\Psi}{\sqrt{1+V_p^2}}$
6. Clocks stationary, mass moving radially				$\frac{d\tau}{dt} = \Psi \sqrt{\frac{1+V_p^2}{\Psi+V_p^2}}$
7. Clocks stationary, mass moving transversely				$\frac{d\tau}{dt} = \sqrt{\Psi}$

Note  $\Psi = 1 - \frac{2m}{r}$   $V_p = \text{local velocity} = \frac{dx}{d\tau}$  Mass,  $m$ , has Schwarzschild radius  $R_s = 2m$

**Figure 4.** Relative time dilation in Schwarzschild gravity for local ( $2m < r < \infty$ ) and remote ( $r \rightarrow \infty$ ) clocks under various limiting circumstances. Time dilation for stationary clocks in the presence of a moving mass depend on the velocity and direction of the black hole's motion.

time dilation within the plane of the ring is first considered. By symmetry, the only independent coordinate is the radius  $r$  and the time dilation  $d\tau/dt$  at that point is approximated by:

$$\frac{d\tau}{dt} = \sqrt{1 - \frac{2abG}{c^2} \int_0^{2\pi} \frac{d\phi}{\sqrt{r^2 + a^2 + 2ar \cos \phi}}} \quad (40)$$

Setting  $\varphi = \phi/2$  the time dilation can be expressed in

terms of a complete elliptic integral of the first kind,  $K(k)$ :

$$\frac{d\tau}{dt} = \sqrt{1 - \frac{8abG}{(a+r)c^2} \int_0^{\pi/2} \frac{d\varphi}{\sqrt{1 - k^2 \sin^2 \varphi}}} \quad (41)$$

$$\text{or } \frac{d\tau}{dt} = \sqrt{1 - \frac{8abG}{(a+r)c^2} K(k)} \quad \text{where } k = \frac{2\sqrt{ar}}{a+r} \quad (42)$$

The point at the centre of the ring ( $r = 0$ ) is a special

case which is readily integrated to give:

$$\frac{d\tau}{dt} = \sqrt{1 - \frac{4\pi bG}{c^2}} \quad (43)$$

In order to describe a TBH, the ring density  $b$  must be smaller than  $c^2/4\pi G$ . By writing  $(\sqrt{a} - \sqrt{r})^2 \geq 0$  and expanding it is found that  $k \leq 1$  in all cases of (42) satisfying the requirements of the elliptic integral,  $k$  being the ratio of the geometric and arithmetic means of the parameters  $r$  and  $a$ . For the static case, the term within the square root becomes zero at the event horizon. If rotation is allowed, the time dilation will become infinite not at the event horizon but at the static limit, the external boundary of the ergoregion where the invariant interval of motionless particles is lightlike.

When the ring singularity rotates with constant angular velocity  $\omega$ , the velocity of a point on the ring is taken to be  $v_r = a\omega$ . Consider the component of this velocity directed towards the observer  $P$  situated at some radius  $r$  from the centre of the ring and within the equatorial plane. This component contributes to the time dilation experienced by the observer according to the expression presented in condition 6 of Fig. 4. The terms within the square root causing a deviation from parity of proper and coordinate time are once more summed. The ring's total mass  $2\pi ab$  as before. Assuming the centre of mass to be located at the centre of symmetry, the following estimate of the ring's angular velocity shall be used:  $a^2\omega^2 \approx 2\pi bG$  so that the angular velocity is  $\omega \approx \sqrt{2\pi bG}/a$ . Recalling the expression for time dilation of condition 6 and substituting  $\psi = 1 - (2m/r) = 1 - r_+/r$  then rewriting in such a way as to give a separate and integrable deviation from unity within the square root gives:

$$\frac{d\tau}{dt} = \psi \sqrt{\frac{1+v_p^2}{\psi+v_p^2}} = \sqrt{1 - \frac{r_+}{r} \left[ \frac{(1+2v_p^2) - \frac{r_+}{r}(1+v_p^2)}{1+v_p^2 - \left(\frac{r_+}{r}\right)} \right]} \quad (44)$$

As  $r \rightarrow r_+$ ,  $d\tau/dt \rightarrow 0$  which means only particles travelling at the speed of light can remain on the horizon, as expected. As it stands, this formula allows the deviation from unity within the square root to be summed for an arbitrarily large number of point masses, regardless of the mass contained by each. Simplification is possible if it is assumed that all these point masses are infinitesimally small so that the Schwarzschild radius of each is negligible compared to the distance between each mass and the local clock where  $d\tau/dt$  is to be determined,  $r_+ \ll r$ . Implementing this simplification and including the integration symbol to emphasise the fact that the point masses should be vanishingly small yields:

$$\frac{d\tau}{dt} = \sqrt{1 - \int \frac{r_+}{r} \left( \frac{1+2v_p^2}{1+v_p^2} \right)} \quad (45)$$

The time dilation relative to observers at spatial infinity is now derived for points surrounding the rotating ring singularity. These test points are assigned cylindrical coordinates  $(r, \phi, z)$ , and are not confined to the equatorial plane. By symmetry the  $\phi$  coordinate is redundant. The resulting time dilation resembles the previously derived expression containing an elliptic integral but with additional complexity:

$$\frac{d\tau}{dt} = \sqrt{1 - 2ab \int_0^{2\pi} I(\phi) d\phi} \quad (46)$$

substituting  $u = a^2 + r^2 + z^2$  the integrand reads:

$$I(\phi) = \frac{u + 2ar \cos \phi + 2a^2 r^2 \omega^2 \sin^2 \phi}{\sqrt{u + 2ar \cos \phi} (u + 2ar \cos \phi + a^2 r^2 \omega^2 \sin^2 \phi)} \quad (47)$$

Note that the time dilation at the centre of the ring ( $r = 0, z = 0$ ) is still given by (43) because the velocity of each point mass is perpendicular to the line connecting the point mass to the local observer and that this holds along the entire axis of rotation. It would be possible, but more complicated, to determine the approximate location of event horizons using a similar method. One would need to transform the local observers to those of a locally non rotating frame (LNRF). This would be achieved in the equatorial plane by relating the angular velocity of the ring to that of the local observers. Starting with condition 6 of Fig. 4, one would generalise to the case where the local clock and point mass have separate (non-zero) velocities with respect to the clock at spatial infinity by applying a Lorentzian boost to the coordinate clock. Then, equivalents to the expression in (43) and (45) would need to be found.

The time dilation can be computed numerically but care is needed when selecting the ring's angular velocity  $\omega$  otherwise the situation becomes unphysical with frame-dragging velocities in excess of  $c$ . This formula was used to determine the shape of the ergoregion in Fig. 3 when viewed in cross section. Fig. 5 presents a 3-dimensional projection of the time dilation as viewed by observers located at spatial infinity for the equatorial plane intersecting a rotating TBH. This embedding diagram portrays local time dilation (as viewed by distant observers) due to the presence of mass as the deviation from an otherwise flat plane according to (47). The TBH drags local spacetime with it in synchrony with the event horizon. Accordingly, inertial test particles travelling within the equatorial plane along initially radial geodesics from spatial infinity are compelled to orbit the TBH until their angular velocity reaches that of the event horizon. This occurs at the moment the horizon is crossed. Colour is used to denote the angular velocity of locally non-rotating observers as measured by distant observers, colours of longer wavelengths representing angular velocities approaching that of the TBH. A section of the outer funnel has not been plotted to provide visibility of the TBH aperture region. The ergoregions have not been identified here.

## 6 JET FORMATION FROM TOROIDAL BLACK HOLES

The near-maximally rotating TBH undergoing accretion provides an excellent mechanism for the formation of ultra-relativistic (Lorentz factor  $\sim 10$ ) bi-directional jets as have been observed in quasars. The purpose of this section is not to explore the behaviour of the jets as they travel towards the distant radio lobes, the magnetohydrodynamics of which has been studied in great detail elsewhere, nor to analyse the myriad of particle interactions capable of extracting rotational energy from the TBH ergoregion. Rather, the essential differences between existing models and the accretion of matter onto a rotating TBH shall be outlined. Supermassive BHs have long been thought to reside at the heart of quasars and active galactic nuclei. Though masses as large as  $10^9 M_\odot$

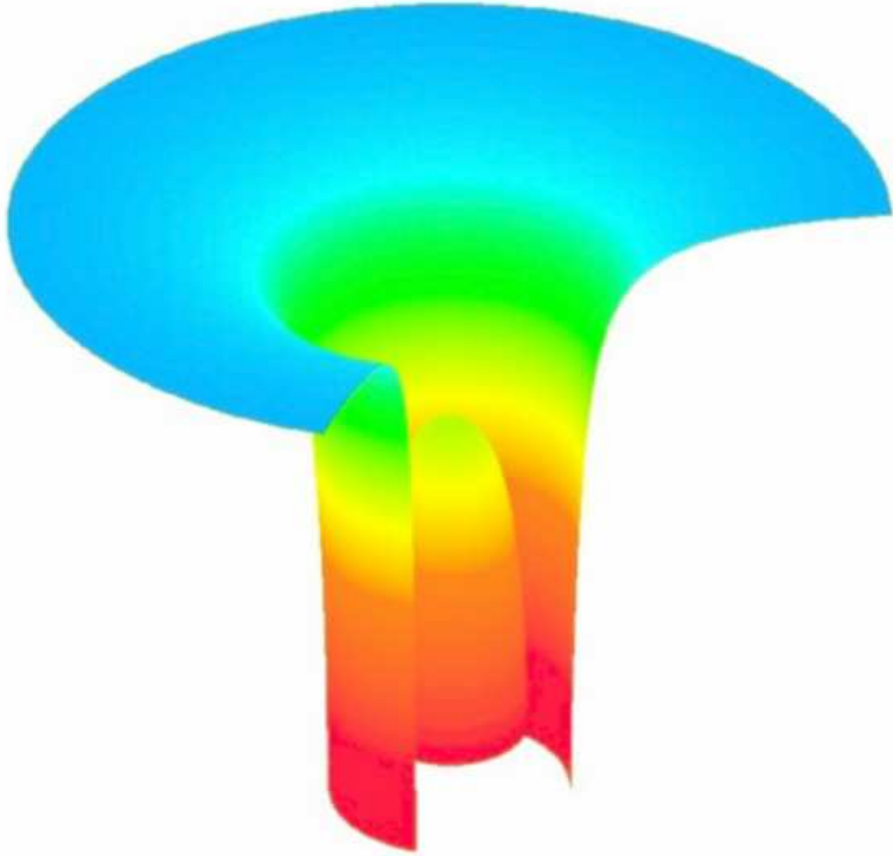


**Figure 5.** Embedding diagram for the simulated time dilation within the equatorial plane of a rotating TBH. A portion of the outer funnel has been omitted revealing the central aperture. The rotation rate in equilibrium cannot be precisely estimated, but for any given toroidal geometry, relativistic rotation acts to enhance the time dilation at all locations except the axis of rotation axis.

have been associated with these, a typical rotating galaxy possesses ample angular momentum to spin up BHs of this size to maximal rotation. An upper limit on rotational velocity exists because the peak velocity of the event horizon cannot exceed that of light. In practice, the maximum rotation rate will not be reached, not least because the internal singularity would be revealed. Transportation of angular momentum away from the TBH by jets imposes more practical limitations. Hence the formation of jets, an intriguing feature of many AGN, is of paramount importance. Potential mechanisms responsible for their origination are now presented within the framework of the TBH model.

A nascent galaxy may harbour a TBH whose spin rate is increasing. Once the spin reaches a plateau after a short delay (in cosmological terms), equilibrium is achieved and the accretion process is balanced by the angular momentum released by the TBH due to gravitational radiation, the production of jets and growth through capture of mass and angular momentum. Of these, the outflow of angular momentum is typically dominated by jet generation processes. This maintains a rapidly rotating TBH, but implies that accreting matter rotates with greater angular velocity than the spacetime near the TBH. Essentially, the interaction between this accreting mass and the enormous fly-

wheel of the rotating TBH constitutes the basis for jet energy release. Fig. 6 illustrates a rotating TBH surrounded by an accretion disk. Since the TBH is able to shed any excess angular momentum by several mechanisms, its angular velocity is suppressed relative to the accretion disk  $\omega_{tbh} < \omega_{disk}$ . Apart from gradual mass accumulation, one can picture the TBH as being largely unaffected during periods of sustained activity, acting somewhat like a catalyser for the expulsion of angular momentum along the jet axis. Jet formation can therefore progress for substantial periods of time:  $10^6 \sim 10^9$  yrs.

Within the central aperture, spacetime is dragged in concordance with TBH. The central aperture is a negative gravitational potential well, a spacetime vortex containing deeply negative energy states. Matter negotiating this central aperture will be obliged to travel along geodesics which appear to the external universe to be rotating. Particles capable of escaping to infinity require relativistic velocities closely aligned to the axis of rotation. Matter is able to travel in either direction along the rotational axis in order to achieve this, and angular momentum is transported away from the TBH equally by each jet. Of primary interest is a TBH whose central aperture is sufficiently small to provide powerful, collimated jets.

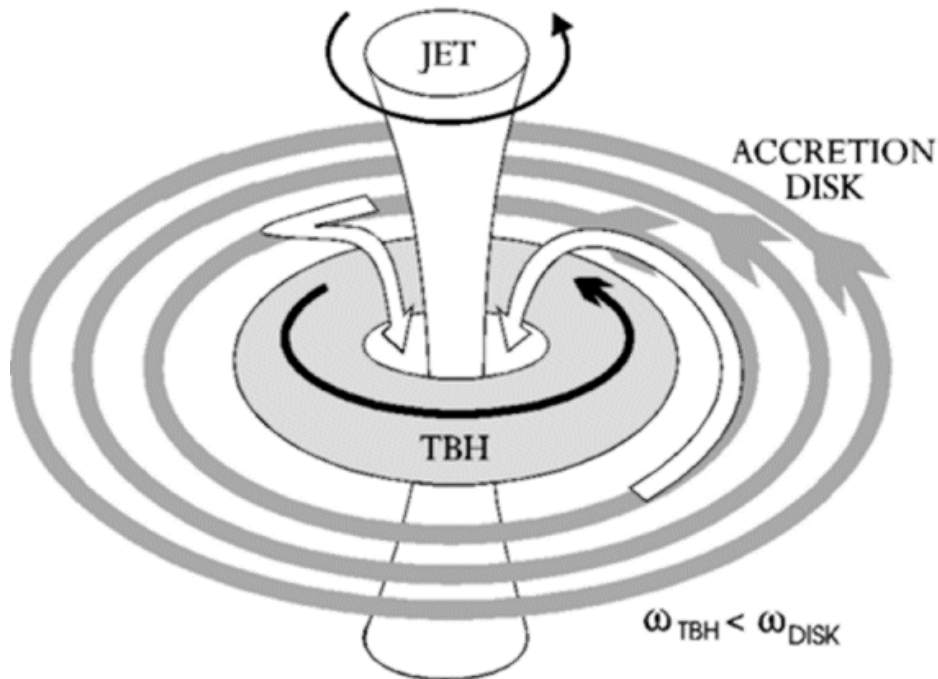


**Figure 6.** The transport of angular momentum in AGN. Rotational energy is supplied by the accretion disk to the TBH which is efficiently redistributed along axial jets by magneto-rotational mechanisms maintaining (i) the angular velocity differential between the TBH and accretion disk and (ii) the net charge on the TBH.

Matter travelling through the aperture will undergo gravitational slingshot and could be propelled outwards along the jets, however the importance of this will be to impart kinetic energy leading to frictional heating. Temperatures of at least several million degrees (and perhaps as much as  $10^{11}$ °K) will be realised in the aperture, transforming the contained matter into a plasma emitting X-rays and some gamma rays.

Ejection mechanisms such as the Penrose process (Penrose 1969), superradiant scattering (photonic counterpart of the Penrose process) and their analogues (e.g. due to particle-particle collisions) could dominate in the formation of jets. For convenience, the term Penrose process is used loosely to refer to all variations. The Penrose process exploits the existence of negative energy orbits inside the ergoregion of a rotating BH, permitting the extraction of energy to infinity at the expense of the rotational/kinetic energy of the BH. A particle travelling through the ergosphere might disintegrate into two particles, one of which plunges headlong towards the event horizon whilst the other emerges from the ergosphere and escapes to ‘infinity’, e.g. as part of a jet. Energy is extracted if the emergent particle fragment has more energy than the originally intact particle, with the captured fragment carrying negative energy into the BH. The Penrose process efficiency improves if the particles have relativistic incident velocities, particularly those opposing the BH’s rotation. A physical example of particle disintegration occurs within a high energy plasma when neutral hydrogen atoms are stripped of their electrons. More generally, ergoregional particle-particle collisions in which angular momentum and total energy are conserved may cause one of the resultant

particles to be ejected to infinity (Piran, Shaham & Katz 1975; Piran & Shaham 1977). Particles are always ejected in a way that reduces the BH’s angular momentum and rotational energy which increases the surface area of the event horizon, in keeping with the entropy law. As has been described by Wagh, Dhurandhar & Dadhich (1985) and Bhat, Dhurandar & Dadhich (1985) the presence of an electromagnetic field and/or charged particles can dramatically increase the efficiency of the Penrose process, easily to a level where net rotational energy may be extracted from the BH.

The astrophysical significance of the Penrose process has been traditionally questioned, partly because BHs of spherical topology are not expected to retain significant electrical charge. It is argued that tori exhibit a vital difference. When a rotating torus accumulates charge, the circulating current establishes a poloidal magnetic field. Lines of magnetic flux encircle the torus but nowhere intersect its surface. Nearby the surface, flux lines are orthogonal to the current flow and parallel to the surface itself. Sufficiently intense magnetic fields constrain the motion of accreting plasma, obliging its constituent particles to follow helical trajectories which wind about lines of flux. Whereas charged spheroids are rapidly neutralised by plasma guided directly towards the surface by flux lines, neutralisation of charged tori is strongly inhibited due to the absence of flux lines intersecting the surface.

According to the membrane paradigm, one can imagine the TBH’s (infinitesimally stretched) event horizon to be an electrically conducting surface where electric fields incident to this membrane are terminated by an appropriate surface electric charge density. Also, the surface current will be such

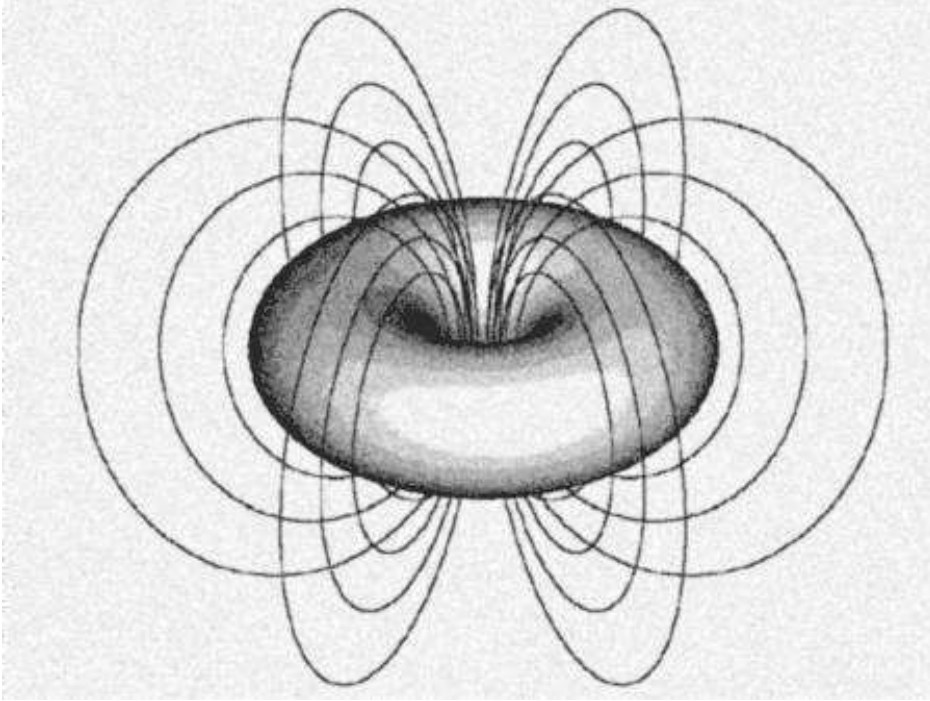


**Figure 7.** The magnetic field originated by a charged, rotating torus. The topology ensures that lines of magnetic flux never intersect the surface - therefore individually charged particles of the accretion disk spiral along the flux into the central aperture without neutralising the torus - in contrast, charged spheroids are easily neutralised since flux always terminates at the surface, typically in polar regions.

that the magnetic field parallel to the surface is terminated, in this way there will be no parallel magnetic field inside the event horizon. The effective surface resistivity will be of the order of several hundred ohms. The accreting matter contains neither magnetism nor net charge initially. The TBH is, however, spinning and dragging local spacetime around with it. The charged particles entering the ergoregions are mainly electrons and protons. Low efficiency Penrose processes will preferentially eject particles of larger charge/mass ratios (the electrons) and a net positive circulating charge will emerge hovering above the horizon. The toroidal membrane rotates and drags these positive charges around with it thus forming a circular electrical circuit. Current flowing in the circuit gives rise to an axial magnetic field through the central aperture, modulating the efficiency of particle emissions via the Penrose process thereby reinforcing the circulating charge and magnetic field. This magnetic field also plays a role in collimating the jets as they are launched, with charged particles spiralling along the magnetic field lines generating synchrotron radiation. Similarly, the dipolar magnetic field of the TBH channels free charged particles from the outer accretion disk into the central aperture, spiralling along the lines of magnetic flux.

The structure of the magnetic field encompassing a conducting toroidal shell is shown in Fig. 7. Lines of flux are illustrated which arise when a current circulates around the toroidal shell. Because the aperture can become arbitrarily small, if the total charge of the torus remains constant, the flux density and hence magnetic field can become arbitrarily large within this region. Computed plots of magnetic field strength along the equatorial plane of the torus are given for four separate toroidal geometries in Fig. 8(a). These have

been calculated using the usual Biot-Savart relations and assume a constant and uniform surface current density  $J$ . Analytically, the magnetic field strength perpendicular to and within the equatorial plane at some displacement from the axis  $a$ , making use of symmetry, is given by the double integral:

$$B(a) = \int_0^{2\pi} \int_0^{2\pi} \frac{\mu_0 J t (a \cos \phi - t \cos 2\phi)}{4\pi (a^2 + t^2 + R_2^2 \sin^2 \vartheta - 2at \cos \phi)^{3/2}} d\phi d\vartheta \quad (48)$$

where  $t = R_1 + R_2 \cos \vartheta$  (49)

The Biot-Savart law simplifies at the centre of a circular current loop carrying a current  $I$  and it is straightforward to verify that the field strength at that point is:

$$B(0) = \frac{\mu_0 I}{2R_1} \quad (50)$$

Nearby the toroidal surface, Ampere's circuital law (51) states that the current enclosed by a closed path determines the sum of the magnetic field along the same closed path so the field strength is always finite at the shell's surface.

$$\oint B ds = \mu_0 \times I \quad (51)$$

The same law demonstrates that the integral (48) is independent of  $R_2$  providing  $a < R_1 - R_2$  or  $a > R_1 + R_2$ , therefore some simplification is available by setting  $R_2 \rightarrow 0$  whilst a constant current circulates. The integral of (47) can be expressed in terms of multiple elliptic integrals. Numerical computations have been used to derive plots in Fig. 8(a) which show that the field within the central aperture is generally stronger than in the outer periphery of the torus as measured by local inertial observers. This is particularly true for the geometries where  $R_2 \rightarrow R_1$  that would produce

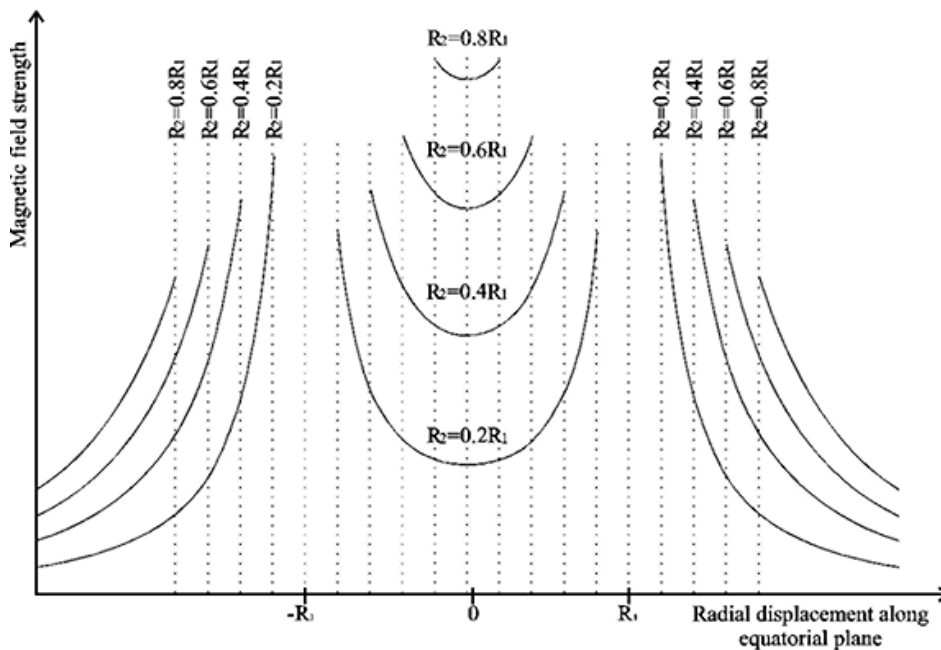


**Figure 8. a)** Magnetic flux density in the equatorial plane of a rotating, charged toroidal shell for four separate geometries. The flux density can become arbitrarily large within the central aperture as the minor radius of the torus approaches the major radius.

tightly collimated jets. The charged particles spiral around the strong field lines of the aperture achieving high velocities and alternate between contra-rotation and co-rotation during each cycle of their spiral. During the contra-rotation phase, they are especially likely to participate in ergoregional particle collisions in which energy and momentum is transferred to the jets at the expense of the angular momentum of the TBH.

To better approximate the magnetic field of a charged TBH, the gravitational time dilation must be taken into account. Restricting analysis to the time dilation generated by a momentarily static ring singularity whose event horizon is transiently toroidal, the horizon must coincide in the equatorial plane with the surfaces of the electrically conducting toroidal shell. Essentially, this is achieved by precise adjustment of the radius of the ring singularity ( $R_{ring} > R_1$ ) and the ring singularity's mass per unit length. The magnetic field strength plots of Fig. 8(a) are then recalculated, this time taking account of the local time dilation (lapse function) relative to a distant observer. The situation is analogous to earth based quasar observations because this magnetic field directly modulates the non-thermal radiation emanating mainly from within the TBH ergoregion. Note also, the negative energy states within the ergoregion of the central aperture will be more negative than elsewhere within the ergoregion but that the increased time dilation counteracts this. Results are presented in Fig. 8(b). Again, the electrical surface current density  $J$  has been held constant but the TBH mass is different in each case.

Several factors need to be considered which potentially impact the results. Time dilation diminishes more rapidly than flux density with axial displacement. Improved models would involve non-uniform surface current densities for the TBH membranes, a means of estimating the TBH charge

and a more accurate determination of the TBH angular velocity, which may require a theory of quantum gravity.

These facts imply that the Penrose process will occur predominantly within the central aperture of the TBH, and less so in the outer regions. Ergoregional particle emissions in the outer regions are largely reabsorbed by interactions with the accretion disk, whereas the rarefied central aperture allows relatively unimpeded passage to scattered particles. Thus, the most visibly energetic TBHs will be those with tightly focused jets.

As discussed previously, because charge neutralisation is inhibited for tori, intrinsically stronger magnetic fields are to be anticipated in the vicinity of a TBH as compared to the rotating spheroidal BH situation. The presence of the magnetic field and the plasma gives rise to a force-free magnetosphere within the TBH's central aperture providing the plasma is sufficiently rarefied. The accumulation of circulating positively charged particles moderated by time dilation nearby the TBH event horizon is, for present purposes, identical to the situation where the TBH itself is charged. Supposing that the equilibrium magnetic field stabilises at large values  $\sim 10^{12}$  G or larger, then vacuum breakdown may play a part in the formation of jets. Energy stored in the TBH magnetosphere would then be tunnelled quantum mechanically, creating pairs of charged particles and anti-particles. These virtual particles would then be separated by the intense electromagnetic forces before they could silently annihilate one another. The detection or otherwise of a significant positron population in the jets is a useful tool for resolving the issue of whether vacuum breakdown has a role to play.

Energetic photons (X-rays and gamma rays) generated by the plasma of the central aperture would be emitted in all directions. Ergoregional processes would be capable of promoting them to higher energies because they are trav-

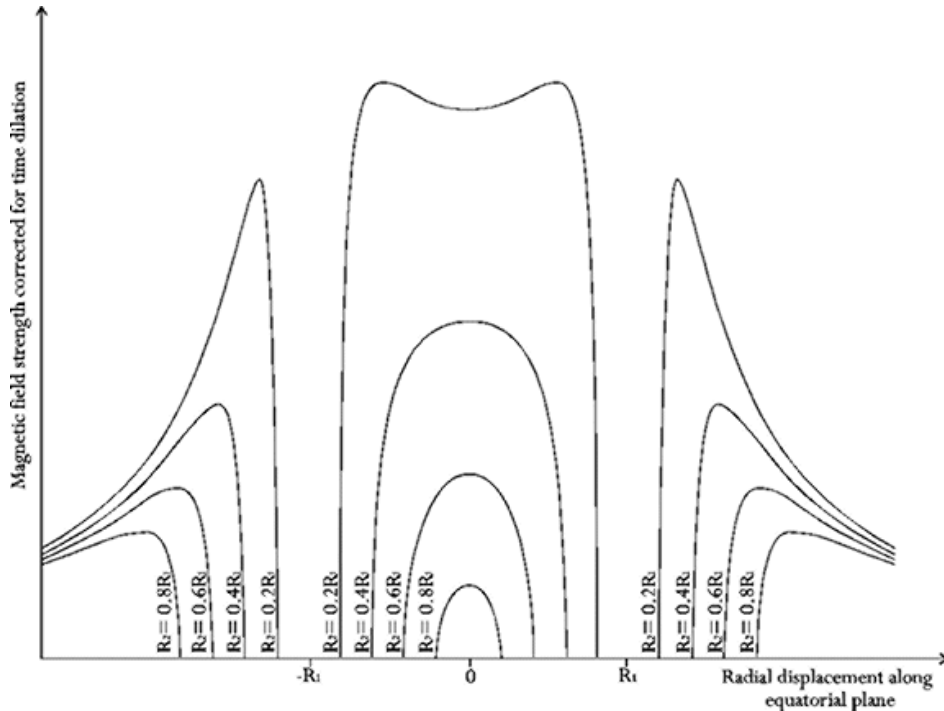


**Figure 8. b)** Magnetic flux density corrected for time dilation in the equatorial plane of a conservatively under-rotating, charged TBH for four geometries. More realistic, rapid rotation does not affect the time dilation along the axis of rotation but can boost the time dilation elsewhere, resulting in maximal effective flux densities located in the central aperture for all cases.

elling at the speed of light, often in retrograde trajectories about the TBH. Resulting photons could inhabit the gamma ray spectrum at energies as high as the TeV range. The Penrose process should also act on the high velocity electrons and atomic nuclei of the high-energy plasma occupying the ergoregion of the aperture. At the expense of the rotational energy of the TBH, bi-directional jets with relativistic velocities are therefore likely to result. Matter and radiation must necessarily emerge from either side of the central aperture, where it begins its journey along one of the two jets. Depending on the geometry of the TBH, the jets could be tightly focused and penetrating or conversely, spluttering weakly over a broad solid angle. Particles are preferentially ejected in close alignment with the modulating magnetic field, in this case along the spin axis of the TBH. The toroidally originated magnetic field provides for deeper negative energy states within the ergoregion whilst extending the region of occurrence well beyond the static limit surface. Bhat, Dhurandar and Dadhich demonstrated that when charged particles are involved in Penrose process interactions there exists virtually no upper bound on the efficiency of energy extraction.

The jets are to some extent able to collimate themselves if they are sufficiently focused at the source by trapping the magnetic field internally. Magnetohydrodynamic studies have had much success in explaining the characteristics of these outflows which emerge supersonically and travel for several millions of light years before ploughing into radio lobes formed at the ICM/jet interface. The knots frequently visible along jets are readily interpreted as the result of substantial short-term matter ingestion from stellar collisions with the TBH or instabilities in the accretion flow, one fur-

ther possibility being that these knots may also be related to rapid fluctuations in TBH charge and instabilities in the TBH mechanism itself. The rotating jets will cause a net outflow of angular momentum from the TBH, which is counter-balanced by the net inflow of angular momentum due to accretion around the TBH's periphery. Jets transport angular momentum from the TBH because particles ejected from the ergoregions are rotating with the TBH having been launched by the Penrose process within the ergoregion, thereby generating a decelerational torque (recoil) on the TBH. By the mechanisms described, a significant portion of the mass and kinetic energy of accreting matter and radiation is available for jet production. For detailed analysis, numerical simulations will be required.

The Penrose process reaches maximum efficiency when one of the particles heads directly towards the event horizon along the shortest path (i.e. it has the most negative energy state possible). Similarly, when the negative energy state arises due to the presence of charge on a particle, one of the particles emerging from the collision ideally scatters towards the event horizon along the shortest path. When the trajectory of the other scattered particle is considered for the purely gravitational Penrose process, the particle will head directly away from the event horizon, which for the TBH central aperture is typically a poor escape route. The situation is altered for electromagnetically dominated Penrose process interactions as the potential of the charged particle within an electric field should be considered. In order to recoil with maximal energy extraction, the charged particle will follow a path that leads towards greatest electrical potential which, for the aperture of a charged and rotating TBH, is aligned axially with the magnetic field. These

ejected particles will frequently collide with the accretion flow streaming from the outermost periphery of the TBH. The jets will be sufficiently strong to overcome this inward accretion flow in the regions nearest the spin axis. An almost identical scenario was analysed (Blandford & Rees, 1974) wherein hot, relativistic plasma escapes anisotropically through orifices punctured in a cool surrounding gas resulting in beams of collimated plasma.

Data gleaned from quasar observations is consistent with the present TBH model. High energy gamma rays at energies up to 20 GeV  $\sim$  1 TeV have been detected within the jets. These may correspond to photons ejected by the Penrose process, rather than by some secondary acceleration mechanism within the jets. The variation in jet dispersion angles is related to the  $R_2/R_1$  ratio of the TBH and is naturally accounted for by the opening angle of the TBH. Quasar spectra can contain three separate red-shifted portions; the TBH model displays a similar complexity:

- The plasma of the central aperture is buried in a deep gravitational potential well.
- Jets travel relativistically in opposite directions, one of which is usually not directly detectable.
- Radiation passes through the metal enriched clouds generated by the SN of the TBH creation event.
- The remoteness of the QSO galaxy correlates to a cosmological recession and red-shift.

A carefully considered numerical study of gravitating fluids (Marcus, Press & Teukolsky 1977) reveals a bifurcation from the Maclaurin ellipsoids to lower energy state 'Maclaurin toroids' at high angular momenta which the authors suggest may be stable against all small perturbations. Alternatively, toroidal density distributions (TBHs or transient neutron tori) may develop in the dynamically collapsing cores of moderately rotating progenitor stars (rotary core collapse). Butterworth & Ipser (1976) demonstrated that ergoregions can form when relativistic stars spin rapidly although absolute event horizons are absent. With the notable exception of long-term stability, charged neutron tori could share many similarities with the charged TBH central engine of quasars. Although the neutron torus could exhibit various non-axisymmetric instabilities, it appears that the electromagnetic structure could significantly counteract these effects for core-collapse timescales if electrical charge gathers on the torus. Moreover, stability will clearly be reinforced if the composition of the torus becomes superfluidic and superconducting, as is likely for the least soft equations of state.

Rotating, electrically charged neutron tori are able to generate immensely strong axial magnetic fields. When ergoregions arise and accreting matter is available, relativistic bi-directional jets should emerge. Given a steady supply of mass and angular momentum, as from an accretion disk fuelled by a binary companion star, microquasar behaviour could result — though long-term stability arguments favour a TBH engine. Certain explosive core-collapse SNe (hypernovae) accompanied by anisotropic gamma-ray bursts (GRBs) could be interpreted as the outcome of a neutron/BH torus forming during rotary core collapse. Metastable configurations can be envisaged in which a white dwarf accretes matter from a companion star, the angular momentum accumulates until the core eventually collapses

to a neutron torus causing a brief but intense outburst of mass and angular momentum sufficient for the star to resume its quiescent spheroidal white dwarf state. Recovery from neutron to white dwarf densities is permitted, but event horizons grow irreversibly. Rotary core collapse may curtail the birth of TBHs at masses substantially *below* the lower limits commonly adopted for BHs.

## 7 EVOLUTION BEYOND OPTICALLY BRIGHT QSO PHASE

It is well documented that quasar populations decline rapidly at co-moving red-shifts below  $z \sim 2.5$ . What is not easily explained by leading models reliant on a central supermassive spheroidal BH is why quasar activity terminates so abruptly in recent times. This is especially puzzling given that the BHs themselves cannot have altered other than gain yet more mass from their surroundings. Ideas have been proposed such as advection dominated accretion flow (ADAF), the 'spin' paradigm and various 'state transitions' related to accretion efficiency. A significant diminution of BH angular momentum is unlikely given the tendency of accretion disks to transfer rotational energy to a BH. If fundamentally different modes of accretion do operate, lower efficiency modes will be obliterated whenever a massive body approaches the disk/engine environment. Mass injection of this kind would sporadically re-establish brief quasar behaviour in previously dormant galaxies, including neighbouring galaxies which are observed to be emphatically inactive. Evidence for such transient activity is absent both in local and distant galaxies. This is exceedingly troublesome for standard AGN models when accounting for the quiescent cores of nearby giant ellipticals.

According to the present model, the TBH will transition to a spheroidal BH once accretion has inflated the event horizon or decreased the angular momentum sufficiently. This provides a natural mechanism for the termination of quasar-like TBH activity within the universe and is amply supported by observations. The swelling of the toroidal event horizon due to mass capture generally overcomes the increasing angular momentum of the TBH by the same process. Although the major radius of the torus may be increasing, the minor radius will eventually catch up leading to a topological transition. Immediately prior to the extinction of the TBH, the most energetic and tightly collimated jets are anticipated to form, albeit with enhanced gravitational red-shifts as seen from infinity.

Fig. 9 illustrates a number of features of the TBH quasar model and has been constructed using the inequality relations (12) to (15) from section 2. The shaded wedge represents the area within which TBHs can come into being directly from the implosion of a toroidal star. Here, it has been assumed that the seed star has constant density of  $\sim 1400 \text{ kg m}^{-3}$  and that 90% of the star's mass is ejected during the implosion ( $\eta = 0.1$ ). TBH creation at radii  $R_1$  below about  $36 \times 10^9 \text{ m}$  is prohibited because electron or neutron degeneracy would halt the collapse, as it would slightly beyond the left hand edge of the diagram at about  $R_2/R_1 \sim 10^{-6}$  and beyond, so that the wedge shape does not continue indefinitely. Above the shaded wedge, it is impossible for the toroidal star to be sufficiently massive if, as

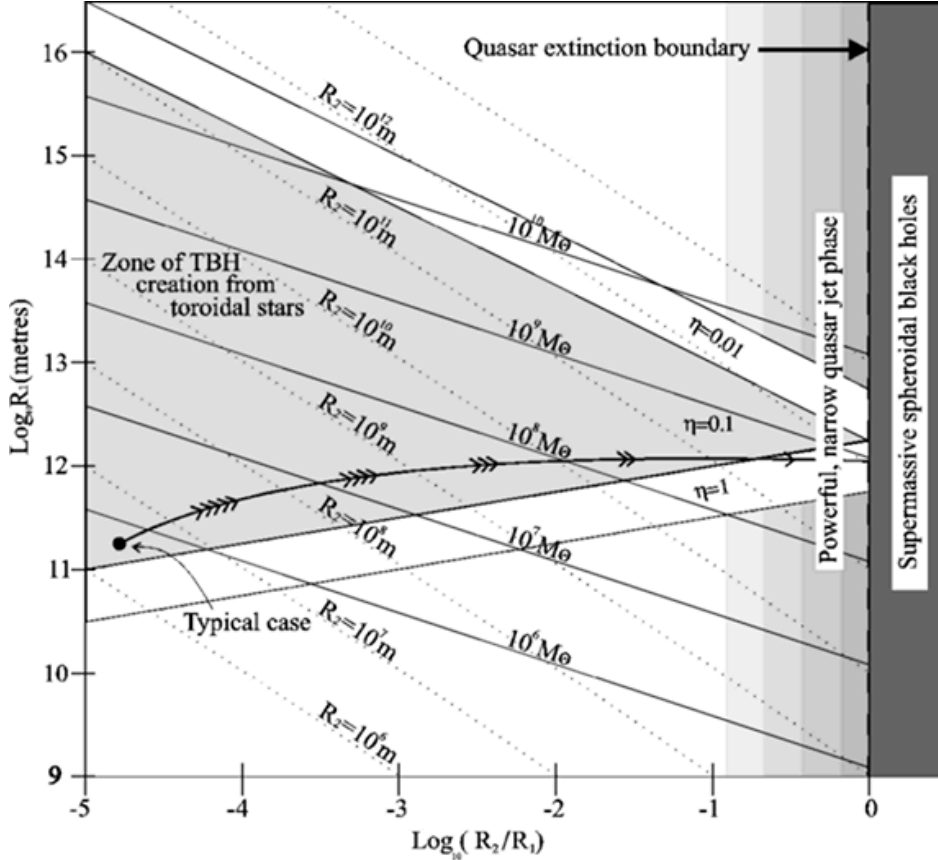


**Figure 9.** Toroidal black hole creation, evolution and extinction. Contours of constant mass can only be traversed in one direction. A typical case is identified which corresponds to the lifecycle of a prototypical quasar. AGN extinction accompanies the topological transition at  $\log(\frac{R_2}{R_1}) = 0$ . Beneath the shaded wedge, TBH formation can occur from the collapse of degenerate tori.

it must be,  $R_3 < R_1$  for the seed star and densities above  $1400 \text{ kg m}^{-3}$  are disallowed. Lightly shaded regions above and below the main wedge show how the diagram would be altered if different values were taken for  $\eta$ .

This diagram identifies the region at which quasar-like behaviour is to be expected from TBHs (progressively shaded vertical section) where  $R_2$  is almost as large as  $R_1$  and narrow jets are formed. The line defined by  $R_2 = R_1$  is the quasar extinction boundary where the TBH becomes a spheroidal BH. Lines have been plotted to indicate contours of equal TBH mass and similarly for constant minor radius  $R_2$ . Because the mass of the TBH will not diminish with time, constant mass boundaries can only be traversed in one direction. There is a sufficiently broad birth zone spanning several orders of magnitude on each axis which enhances the probability that TBH creation is widespread at the centre of typical protogalaxies.

TBH birth is anticipated to occur at lower masses and lower  $R_2/R_1$  ratios because the seed stars required are very large even for these. One typical case has been presented on the diagram. For this example a toroidal star of mass  $6 \times 10^6 M_\odot$  and radii  $R_1 = 1.8 \times 10^{11} \text{ m}$  and  $R_3 = 8.7 \times 10^{10} \text{ m}$  implodes after exhausting its fuel on a very short timescale to leave a TBH of mass  $6 \times 10^5 M_\odot$  and radii  $R_1 = 1.8 \times 10^{11} \text{ m}$  and  $R_2 = 2.8 \times 10^6 \text{ m}$ . The accretion rate within this young galaxy is increasing so the TBH mass swiftly increases as does its angular momentum and angular velocity. The ar-

rows of the evolutionary trace depict the evolutionary rate, fastest at the start then slowing down at higher masses such that the QSO phase can exist for a timescale several orders of magnitude greater than the formation time of the TBH. Somewhat inevitably, when  $R_1$  and  $R_2$  equalize, the quasar phase is discontinued, in this example when the mass reaches about  $10^9 M_\odot$ . For a given mass, the relationship between  $R_1$  and  $R_2$  will depend upon the angular velocity of the TBH which in turn is related to the angular momentum inflow due to accretion. In order to sustain a toroidal event horizon indefinitely, an ever increasing supply of angular momentum may be required. The accretion rate might be relatively low at the time of TBH birth, rising swiftly before peaking and slowly decreasing thereafter. Accordingly, the jet formation phase is predicted to terminate due to the topological transition at the boundary where  $R_2 \rightarrow R_1$ .

## 8 DISCUSSION

It has been qualitatively described how rotating TBHs might evolve from protogalactic gas clouds and accrete matter from the galactic centre until their inner apertures contract and highly focused relativistic jets form. The viability of the model can be tested by observing the evolution of jet collimation with red-shift as this model predicts the degree of collimation continues to increase (though jet energetics

may decline at later times) until the topological transition. Such an approach could further address the issue of whether the entire AGN population or some subset thereof is accounted for by a TBH model. The direct observations of AGN and quasars in our universe suggests that TBHs are more than abstract mathematical constructs. Classical general relativity still remains to be unified satisfactorily with quantum mechanics. Evidently, TBH stability is intertwined with this issue. As direct experiments cannot be performed in intensely curved spacetimes, astrophysical observations must be our guide. The proposed stability of TBHs allows the event horizon's interior to be metaphorically unveiled, providing clues to the nature of quantum gravity and grand unification theories.

General relativity demands that the cosmological constant  $\Lambda$  be sufficiently negative in order to provide long-term TBH stability. Observational estimates of  $\Lambda$  based upon universal expansion reliant on the behaviour of general relativity in weak field environments suggest that its value is very small but probably positive. One possibility is that  $\Lambda$  is primarily a function of local spacetime curvature. Alternatively, the presence of external matter (accretion disk and galaxy) may provide the necessary curvature and non-stationarity permitting TBH stability over indefinite periods.

The TBH model, despite its controversial nature, presents a promising means of understanding the following characteristics of quasars: extreme jet energies, varying jet emergence angles, abrupt extinction, high gamma-ray radiation, the presence of heavy elements and the multiplicity of red-shifts in absorption spectra. None of these features are readily explained by spheroidal BH models. It is encouraging that the TBH model also appears to lead to plausible models for macroscopic processes within supernovae, micro-quasars and gamma-ray bursts. Fortunately, neutron tori – unlike TBHs – are exempt from topological censorship. Hence, these will certainly exist in astrophysical circumstances, if only very briefly. Betraying their existence in distinctive and overtly energetic ways, these curiosities should be amenable to observational identification and study.

Numerical simulations are crucial if accurate comparisons with further detailed observations are to be made. Gravitational wave detectors and planned optical/X-ray interferometer technology will be sufficiently advanced in forthcoming decades to conclusively resolve the question of whether toroidal black holes truly exist.

## ACKNOWLEDGEMENTS

I wish to thank my father, Andrew Spivey for numerous enlightening discussions and continued assistance. Thanks also to Antony Hewish of Cambridge University for initial comments.

## REFERENCES

- Abrahams A.M., Cook G.B., Shapiro S.L., Teukolsky S.A., 1994, *Phys. Rev. D*, 49, 5153.  
 Aminneborg S., Bengtsson I., Holst S., Peldan P., 1996, *Class. Quantum Grav.*, 13, 2707.  
 Bhat N., Dhurandhar S., Dadhich N., 1985, *JA&A*, 6, 85  
 Blandford R.D., Rees M., 1974, *MNRAS*, 169, 395

- Blandford R.D., Znajek R.L., 1977, *MNRAS*, 179,433  
 Brill D.R., Louko J., Peldan P., 1997, *Phys. Rev. D*, 56, 3600  
 Butterworth E.M., Ipser J.R., 1976, *ApJ*, 204, 200  
 Cen R., 1999, *ApJL*, 524, L51  
 Coleman, 1988, *Nucl. Phys. B*, 307, 867  
 Friedman J.L., Schleich K., Witt D.M., 1993, *Phys. Rev. Lett.*, 71, 1486  
 Galloway G.J., Schleich K., Witt D.M., Woolgar E., 1999, *Phys. Rev. D*, 60, 104039  
 Gannon D., 1976, *Gen. Relativ. Gravitation*, 7, 219  
 Ghosh P., Abramowicz M.A., 1997, *A&AS*, 191, 6605G  
 Hawking S.W., 1972, *Commun. Math. Phys.*, 25, 152  
 Hawking S.W., Ellis G.F.R., 1973, *The Large Scale Structure of Space-Time*, Cambridge Univ. Press  
 Holst S., Peldan P., 1997, *Class. Quantum Grav.*, 14, 3433.  
 Huang C.G., Liang C.B, 1995, *Phys. Lett. A*, 201, 27.  
 Hughes S.A., Keeton C., Walker P., Walsh K., Shapiro S., Teukolsky S., 1994, *Phys. Rev. D*, 49, 4004  
 Klemm D., Moretti V., Vanzo L., 1998, *Phys. Rev. D*, 57, 6127  
 Lemos J.P.S., Zanchin V.T., 1996, *Phys. Rev. D*, 54, 3840  
 Livio M., Ogilvie G.I., Pringle J.E., 1999, *ApJ*, 512, L100  
 Louko J., Matschull H.J., 2001, LANL preprint gr-qc/0103085  
 Mann R.B., 1997, *Class. Quantum Grav.*, 14, 2927  
 Marcus P.S., Press W.H., Teukolsky S.A., 1977, *ApJ*, 214, 584  
 Mirabel I.F., Rodriguez L.F., 1999, *Annu. Rev. Astron. Astrophys.*, 37, 409  
 Mirabel et al, 1998, *Astron.Astrophys.*, 330, L9  
 Misner C.W., Thorne K.S., Wheeler J.A., 1973, *Gravitation*, W.H.Freeman & Co, San Francisco, Box 17.2  
 Penrose R., 1969, *Riv. Nuovo Cimento*, 1, Numero Speciale, 252  
 Perlmutter S. et al, 1999, *ApJ*, 517, 565  
 Petkov V., 2001, LANL preprint gr-qc/0104037  
 Piran T., Shaham J., 1977, *Phys. Rev. D*, 16, 1615  
 Piran T., Shaham J., Katz J., 1975, *Astrophys. J. Lett.* 196,L107  
 Shapiro S.L., Teukolsky S.A., Winicour J., 1995, *Phys. Rev. D*, 52, 6982  
 Smith W.L., Mann R.B., 1997, *Phys. Rev. D*, 56, 4942  
 Thorne K.S., 1974, *ApJ*, 191, 507  
 Thorne K.S., Price R.A., MacDonald D.A., 1986, *Black Holes: The Membrane Paradigm*, Yale Univ. Press  
 Vanzo L., 1997, *Phys. Rev. D*, 56, 6475  
 Wagh S.M., Dhurandhar S.V., Dadhich S., 1985, *ApJ*, 290,12  
 Wang L., Howell D.A., Hoffich P., Wheeler J.C., 1999, LANL preprint astro-ph/9912033

## APPENDIX A

General relativity does not restrict the distribution of mass-energy external to event horizons. The question is not whether, but to what extent can toroidal arrangements of neutron degenerate matter be temporarily stabilised by rotation. The purpose of this appendix is to outline and prepare quantitative estimates of the circumstances leading to the creation of neutron tori using extensive simplifying assumptions due to the complexity of the situation. Although it seems that rather extreme conditions are necessary for tori to form, and dynamic evolution could be both violent and rapid, it will be seen that rotary core collapse supernovae are a natural setting for the birth of dense tori. Although the analysis presented is relevant to a broad range of stellar densities, including the formation of toroidal black hole cores, it must be stressed that tori of neutron density and below cannot be instantly dismissed by topological censorship - the primary objection to the formation of TBHs. It is known that ergoregions can form when relativistic stars form with high angular momentum despite the absence of either apparent or absolute event horizons. Potentially, this permits the proposed quasar mechanism to operate in a number of seemingly unrelated astrophysical phenomena.

Many stars, particularly the brighter Type Oe and Be, rotate considerably faster than the Sun. Equatorial velocities in the range  $300 \sim 700 \text{ km s}^{-1}$  are not uncommon as compared to  $2 \text{ km s}^{-1}$  for the Sun. It is thought that the majority of stars have high initial angular velocities but that coupling between solar winds, magnetic fields and the interstellar medium cause a gradual decline in angular momentum. The brighter, more massive stars can be very short-lived and will retain a large angular momentum once their nuclear fuel is spent. It is therefore worthwhile studying the internal structure of rapidly rotating stars undergoing gravitational collapse to determine the conditions best suited for producing toroidal core configurations.

In order to preserve analyticity, a simplified model is presented. Later it will be apparent that removal of any simplifications necessitates a numerical treatment such as the one presented by Marcus, Press & Teukolsky. A uniformly rotating (constant angular velocity) ellipsoid would consist of ellipsoidal shells for which the assumption of uniform shell density is invalidated in situations of interest. Instead, uniformly rotating infinite cylinders are first considered. A cross section is illustrated in Fig. A.1(a) of the proposed structure of a rotating star composed of two immiscible, incompressible fluids with densities  $\rho_1$  and  $\rho_2$  where  $\rho_2 > \rho_1$ . The contours denote lines of equal hydrostatic pressure increasing from zero at the surface of the spheroidal envelope to a peak within the higher density toroidal core.

If the pressure and density within a cylinder composed of two fluids can be shown to reach a maximum at a finite distance from the axis of rotation, Fig. A.1(b), and that such a distribution is in equilibrium, then the some degree of stability can be ascribed to the arrangement in Fig. A.1(a). A Newtonian analysis permits exact solutions by virtue of the superposition of cylindrical shells of differing densities, the linearity of (constant density) cylindrical gravity with radius, the null gravity within infinite cylindrical shells and the gravitational equivalence of cylindrical shells to axial line masses in the exterior regions. Cylindrical coordinates

$(r, \phi, z)$  are employed to consider two immiscible and incompressible fluids of densities  $\rho_1$  and  $\rho_2$  with  $\rho_2 > \rho_1$  rotating smoothly and uniformly. Temperature is neglected because degenerate materials are of particular concern. The gravitational profile is not linear with radius because it is caused by three zones of different density: regions a), b) and c) with radii  $R_1$ ,  $R_2$  and  $R_3$  respectively indicated in Fig. A.1(b). When equilibrium is achieved, the resultant force on each fluid element is zero. In this analysis, the individual forces acting on the elements are due to the pressure gradient, the centripetal acceleration and the gravitational attraction which, by virtue of the cylindrical symmetry, need only be considered in the radial direction. It is elementary to derive expressions for the derivatives of pressure,  $P_a, P_b$  and  $P_c$ , with respect to radius for each of the three regions a), b) and c) respectively:

$$\frac{dP_a}{dr} = r\rho_1(\omega^2 - 2\pi G\rho_1) \quad (\text{A.1})$$

$$\frac{dP_b}{dr} = r\rho_2 \left\{ \omega^2 - 2\pi G \left[ \rho_2 + \left( \frac{R_1^2}{r^2} \right) (\rho_1 - \rho_2) \right] \right\} \quad (\text{A.2})$$

$$\frac{dP_c}{dr} = r\rho_1 \left\{ \omega^2 - 2\pi G \left[ \rho_2 + \left( \frac{R_1^2 - R_2^2}{r^2} \right) (\rho_1 - \rho_2) \right] \right\} \quad (\text{A.3})$$

These expressions are readily integrated using the following boundary conditions:  $P_c(R_3) = 0, P_b(R_2) = P_c(R_2)$  and  $P_a(R_1) = P_b(R_1)$ . It is immediately apparent from (A.1) that the pressure increases with radius from  $r = 0$  providing a certain minimum angular velocity is exceeded:  $\omega > \omega_{\min} = \sqrt{2\pi G\rho_1}$ . For physically meaningful results, the pressure must not become negative at radii occupied by matter. There are two circumstances where this might first arise: at the centre (when the cylinder becomes hollow) and immediately beneath the surface (centripetal forces overcome gravitational forces leading to mass shedding). The latter condition is simply expressed as  $dP_c/dr > 0$  at  $r \rightarrow R_3$  permitting the definition of a maximum angular velocity  $\omega_{\max} > \omega_{\min}$  which is conveniently expressed as:

$$\omega_{\max} = \omega_{\min} \times \sqrt{1 + \left( \frac{\rho_2 - \rho_1}{\rho_1} \right) \left( \frac{R_2^2 - R_1^2}{R_3^2} \right)} \quad (\text{A.4})$$

In general, a wide range of angular velocities are available if the densities are very dissimilar whereas, as the densities of the two fluids approach one another, there is a much narrower range of values that  $\omega$  can occupy above  $\omega_{\min}$ . A specific example is given in which the radii are in the ratio 1:2:3 for  $R_1 : R_2 : R_3$  and the densities 1:2 for  $\rho_1$  and  $\rho_2$ . Results are plotted in Fig. A.2.

The diagram presents the pressure variation along the radius of a rotating infinite cylinder. Several curves have been plotted which correspond to different rates of rotation. For the example given, internal pressure remains positive up to  $\omega \rightarrow 1.155\omega_{\min}$ , the mass shedding limit. The stability of these results is trivial because the assumption of equilibrium was inherent in the model, all solutions are in neutral equilibrium including those at low angular velocity and the non-rotating case. The significance of  $\omega_{\min}$  is that stability cannot be achieved below this if the fluids become infinitesimally compressible because the density and pressure distributions would be qualitatively different.

When a homogeneous rotating cylinder of compressible fluid is considered, it transpires that stability of off-

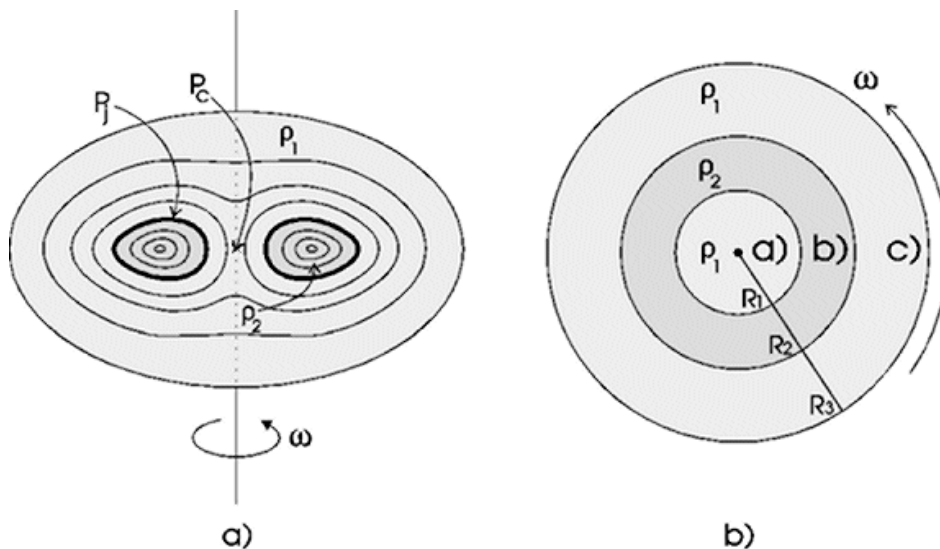


**Figure A.1.** a) A rotating ellipsoid enveloping a denser toroidal core is here approximated by... b) A rotating infinite cylinder (cross section illustrated) composed of two incompressible fluids arranged in a pseudo-toroidal formation where  $\rho_2 > \rho_1$ .

axis peak density arrangements is unattainable if the assumption of uniform rotation is retained. This is evident upon inspection of (A.1) for cases where the pressure and density are positively correlated i.e.  $dP/d\rho > 0$ . This does not mean that an axial pressure-density peak will always result, once the central angular velocity exceeds a certain value  $\omega_c \sim \sqrt{2\pi G\rho_c}$  then axial density peaks are also unstable and differential rotation will occur (non-constant angular velocity). Furthermore, the angular velocity will generally decrease with radius for these systems, coinciding with the most physically realistic situations exemplified by the frame-dragging of the Kerr spacetime. Hence a non-axial density peak akin to toroidal solutions of rotating gravitating spheroids results. A numerical treatment must be employed for systems of even this complexity, before realistic interactions such as viscosity, radiation pressure, temperature variations and magnetic braking are incorporated in the model. Analytical limits of relevance to infinite cylinders exist in (i) the differentially rotating incompressible fluid approximation and (ii) the uniformly rotating compressible fluid regime whereby iterative solution of Volterra integral equations is in principle achievable. Numerical techniques become mandatory for differentially rotating compressible fluids in the infinite cylinder approximation.

It should be stressed that long term stability is not the issue here – all that is required is for a differentially rotating toroidal structure to transiently exist during the inherently dynamic and unstable collapse phase of stellar evolution - the necessary timescale for ‘stability’ is briefer than that required for dissipative processes to restore uniform rotation, e.g. magnetic braking and viscosity.

When a rapidly rotating star collapses, and the collapse originates at the core where gravity first defeats pressure, strong differential rotation accompanies a radial inrush of material - this environment facilitates the formation of a toroidal core. Because angular momentum is conserved for all collapsing shells, the angular velocity in the core increases appreciably to a level in excess of  $\omega_{\min}$  and the angular veloc-

ity beyond the core declines radially. If the core is sufficiently dense, relativistic frame dragging contributes to the differential rotation. Radially decreasing rotation coupled to the fact that the pressure (and therefore the density) must increase with radius at the centre means that toroidal cores are practically inevitable during the collapse of rapidly rotating stars. Axisymmetric tori often exhibit non-axisymmetric instabilities in numerical simulations, the resultant gravitational radiation being of fascination to gravitational wave astronomy. The perturbational influence of orbiting companions could also disturb the symmetry. A simple equation of state is insufficient to model superfluidity and superconductivity, properties that neutron stars are widely expected to possess, rendering inapplicable many models constructed to investigate gravitational wave driven instabilities. The self-gravity of a torus can sustain a state of pseudo-equilibrium. If the torus is electrically charged, the exterior magnetic field acts as a barrier both to surface winds consisting of charged particles and to neutralising inflows – reinforcing stability. The outcome for situations where both  $\omega_{\min}$  and  $\omega_{\max}$  is exceeded is qualitatively unchanged. Mass expelled from the outermost periphery of the torus is not ejected to infinity but forms an equatorial disk orbiting the torus. If sufficient mass is shed, this disk can become geometrically thick, i.e. the torus expands.

For slowly rotating ellipsoids, the value of  $\omega_{\min}$  increases to  $\sim \sqrt{4\pi G\rho_c}$ . If the neutron core following gravitational collapse of the Sun has a density in excess of  $\sim 3 \times 10^{18} \text{ kg m}^{-3}$  then it is conceivable that the core could become toroidal. If a more attainable collapse density of  $10^{14} \text{ kg m}^{-3}$  were specified, then the Sun would only need to rotate at a moderately higher angular velocity of  $\sim 5.5 \omega_{\text{sun}}$  for  $\omega_{\min}$  to be attained during core collapse. The Sun’s internal pressure would first vanish within the surface (mass shed into keplerian orbit) were it to rotate at a rate  $\sim 212 \omega_{\text{sun}}$ , so the available rotation range for toroidal core collapse is generally broad and attainable for typical massive stars.

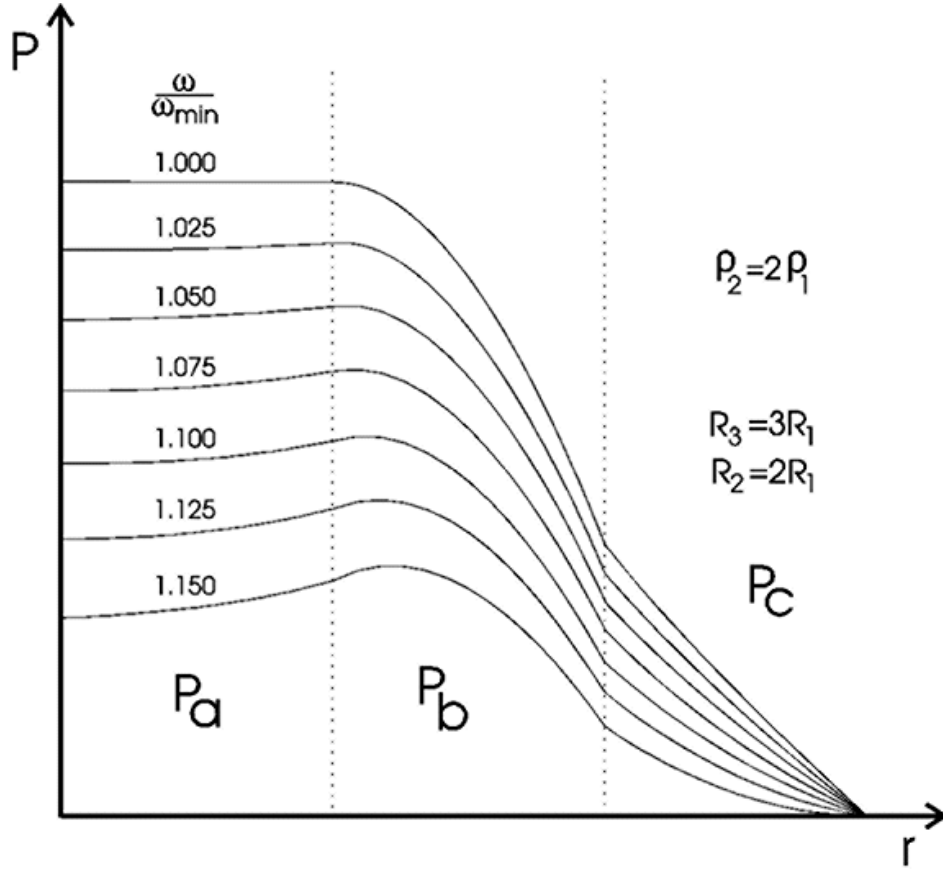


**Figure A.2.** Pressure variation with radius for rotation rates of interest. Quasi-stability occurs for compressible fluids only when the pressure is maximal within region b). At higher rotation rates, mass is shed from the surface into Keplerian orbits.

A TBH embedded in a collapsing stellar envelope resembles a scaled-down version of the described quasar environment. In contrast with the sustained activity of active galaxies, the tremendously accelerated accretion onto the core causes a violent and intense anisotropic explosion. Such a TBH could be of relatively low mass, perhaps below  $0.1M_{\odot}$  as efficient jet generation processes begin to operate and stall its growth. There is therefore a definite possibility that a large fraction of the remaining star is propelled along the jets. Together with the first active galaxies, there are obvious implications for cosmological reionization which appears to have occurred at red-shifts of  $z \sim 6$ . A neutron torus formed during rotary core collapse can ‘recover’ following the ejection of substantial mass from the stellar envelope to a lower density object e.g. a white dwarf. On the other hand, charged neutron tori that do not recover will subsequently collapse to charged spheroidal neutron stars forming highly magnetised pulsars or Kerr-Newman BHs. Objects classified as ‘magnetars’ or anomalous X-ray pulsars (AXPs) have been observed. The inferred magnetic field strengths due to the spin-down rate of these objects is  $\sim 10^{14}\text{G}$ , providing a useful clue as to the degree of electrical charge of the neutron tori during SNe and thus, by inference, the net TBH charge in AGN circumstances. This level of charge can have a significant bearing on the spacetime geometry – this is discussed in appendix B.

White dwarves containing toroidal neutron cores and isolated rotating neutron tori will often form during the core collapse of moderately rotating progenitors. The rotation rate should be sufficient for these dense tori to generate ergoregions thence accumulate charge sustaining magnetospheres which bolster the negative energy states of the ergoregion. These neutron tori are unlikely to be long-lived as they are susceptible to various instabilities and their differential rotation will eventually be erased by dissipative processes, but they are certainly of interest in more dynamic environments. The significance of these short-lived neutron tori or equivalently stellar mass toroidal black holes (SMTBH) are now addressed in three separate astrophysical settings.

Firstly, a binary system consisting of a SMTBH and a stellar companion could operate as follows: an accretion disk forms around the SMTBH composed of material transported from the nearby star by gravitational and electromagnetic interactions. The central aperture of the SMTBH contains an ergoregion and an intense dipolar magnetic field due to a net electrical charge. This then gives rise to anti-parallel jets aligned with the axis of rotation in a very similar manner to the quasar albeit on a smaller scale. Microquasars have been observed within the confines of the Milky Way and are so called because they seem to obey simple scaling laws applied to quasars. Accretion of material from the companion star and jet formation will combine to decrease the overall angu-

lar momentum of the SMTBH on a shorter timescale than that of the quasars, the unusual behaviour terminating when the topology transitions to spheroidal after the angular momentum has been partially jettisoned. Unlike pulsars, the magnetic fields generated by charged tori will be robustly aligned with the rotation axis and, with the possible exception of radiation emanating from an accretion disk, periodic bursts of radiation will not be observed.

Relativistic galactic jet sources and their similarities with quasar outflows have been reviewed by Mirabel & Rodriguez (1999). From the limited microquasar observations available, it appears that the jet velocities have a bimodal distribution classified by  $\nu_{jet} \approx 0.3c$  and  $\nu_{jet} \gtrsim 0.9c$ . Whether a corresponding distribution exists for the jets of active galaxies is currently unknown. An interesting feature of some microquasars which is absent in quasars is their behaviour as the accretion disk is exhausted resulting in a sudden ejection of condensations (Mirabel et al 1998). Existing steady state MHD models with continuous jets have difficulty accounting for this, relying on a disk-supported magnetic field. This problem is resolved in the present model because the magnetic field of the torus remains when the disk disintegrates and confines the remaining plasma to circulate above the event horizon of the SMTBH, weaving repeatedly through the central aperture until it emerges in the form of jets aligned with the spin axis.

Secondly, the mechanism could participate in the most energetic SNe - those which have been dubbed ‘hypernovae’ with energies two orders of magnitude above ‘ordinary’ SNe and thought to coincide with longer duration gamma-ray bursts. GRB980425 has been associated with SN1998bw providing evidence for a common mechanism (Cen, 1999). For example, consider a massive, rotating and fuel starved star undergoing rotary core collapse. A neutron torus (or SMTBH) develops in the core embedded within a lower density envelope. As before, charge accumulates on the torus which cannot be quickly neutralised on a timescale comparable to that of the implosion. A strong magnetic field threads the central aperture of the torus and strongly negative energy states are available in the ergoregion. The mechanism results in a ferocious outward explosion of matter from the centre of the SN in which a significant proportion of the star’s mass is expelled anisotropically. Jets from SNe have been inferred from nearby hot-spots detected by optical speckle interferometry (Cen 1999, and references therein). Evidence of highly anisotropic ejecta is provided by polarimetric SN observations (Wang et al, 1999). Collapsar models attempting to account for jet formation in core collapse SNe are hampered by the spherical core topology as jets, if they form at all, are unlikely to penetrate through imploding shells for the following reasons:

- The inefficiency of the Blandford-Znajek mechanism is now recognised.
- The topology dictates that plasma flowing along magnetic flux lines efficiently neutralises the core — but in the case of toroidal cores, neutralisation paths are orthogonal to flux lines, and neutralisation is thereby inhibited.
- The equatorial plane, which features additional centrifugal forces, is no more unlikely to feature outflows than polar regions if the star is assumed to remain electrically neutral.

Thirdly, pseudo-periodic gamma ray bursts (GRBs) could be generated by a mechanism similar to the microquasar. Consider a rapidly rotating white dwarf with a companion star providing a steady supply of material to an orbiting accretion disk. Metastable oscillations could be established whereby the core of the white dwarf collapses to a neutron torus once sufficient matter and angular momentum has accumulated. This results in a brief period of jet activity in which enough mass and angular momentum is expelled to restore the star to a pure spheroidal white dwarf. Accretion of matter from the binary companion then repopulates the accretion disk, with the mass and angular momentum of the white dwarf slowly increasing until the cycle repeats. It may be that some of the shorter-duration gamma ray bursts can be attributed to situations like this.

## APPENDIX B

A year has elapsed since this paper was deposited on the archive. During that time, explanations for the stability of toroidal black holes have not been ventured. An open discussion along these lines could have been included in the original submission but was not, partly to avoid polarising the views of a sympathetic audience and partly because of the bewildering array of possibilities. Though no claim is made of a satisfactory resolution, this final version devotes an appendix offering a ‘snapshot’ of my thoughts on this issue which have benefited from twelve months of distilled cogitation. Parallels between the Kerr BH and Newtonian analogues comprising a self-gravitating annulus are explored. A simple quantized Newtonian model is used to investigate possible consequences in relativistic settings. The intention is not to denigrate the existing research on black hole spacetimes which has been the focus of much solemn effort by dedicated practitioners of general relativity, rather to communicate some pertinent concerns in a straightforward and hopefully thought-provoking manner.

First it is shown that the ring singularity of the Kerr geometry travels with the velocity of light, regardless of the degree of rotation. Then it is demonstrated that a Newtonian equivalent of the Kerr geometry is a homogeneous self-gravitating ring of infinite density rotating at infinite velocity, implying an unphysically large angular momentum and kinetic energy. This is interpreted as an inevitable consequence of the simplistic model which entirely disregards the microscopic quantum nature of the ring. When a more realistic analysis is pursued in the Newtonian setting, it is observed that the velocity required for equilibrium is logarithmically relaxed - a macroscopically observable consequence of the quantum world. By implication it is then argued that a natural relativistic counterpart deviates from the Kerr solution, and that this deviation would be particularly evident at high angular momenta. Astrophysical environments of interest are then addressed to illustrate the possibility that event horizon topologies may not be restricted to 2-spheres.

In pseudo-Cartesian coordinates  $(\bar{t}, x, y, z)$ , the Kerr metric reads:

$$ds^2 = d\bar{t}^2 + dx^2 + dy^2 + dz^2 + \frac{2mr^3}{r^4 + a^2z^2} \times \left[ d\bar{t} + \frac{(rx + ay)dx + (ry - ax)dy}{a^2 + r^2} + \frac{z}{r}dz \right]^2 \quad (\text{B.1})$$

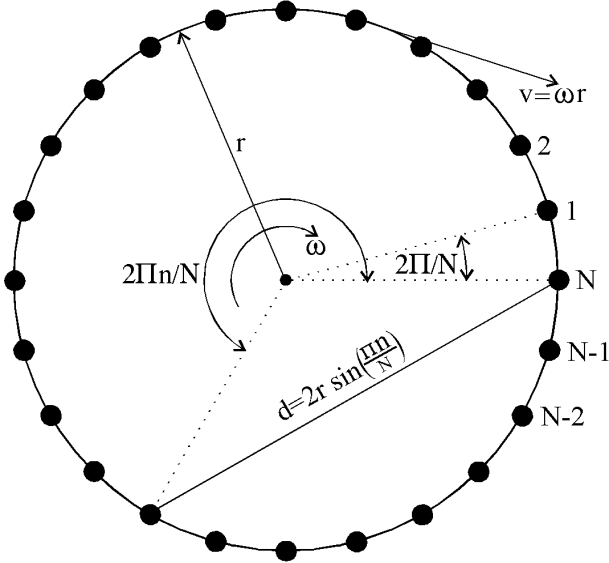


**Figure B.1.** Self-gravitating ring of discrete particles.

and in Boyer-Lindquist coordinates  $(t, r, \theta, \phi)$ :

$$ds^2 = -\frac{\Delta}{\rho^2}(a \sin^2 \theta d\phi - dt)^2 + \frac{\sin^2 \theta}{\rho^2}[(r^2 + a^2)d\phi - a dt]^2 + \frac{\rho^2}{\Delta}dr^2 + \rho^2 d\theta^2 \quad (\text{B.2})$$

$$\Delta = r^2 - 2mr + a^2 \quad (\text{B.3})$$

$$\rho^2 = r^2 + a^2 \cos^2 \theta \quad (\text{B.4})$$

The spatial coordinates of the two metrics obey the transformations:

$$x = r \sin \theta \cos \phi + a \sin \theta \sin \phi \quad (\text{B.5})$$

$$y = r \sin \theta \sin \phi - a \sin \theta \cos \phi \quad (\text{B.6})$$

$$z = r \cos \theta \quad (\text{B.7})$$

A true spherical polar coordinate  $R$ , coinciding asymptotically with  $r$  at large radii, can be defined as  $R^2 = x^2 + y^2 + z^2$  which transforms to  $R^2 = r^2 + a^2 \sin^2 \theta$ . The ring singularity of the Kerr BH resides at  $(r = 0, \theta = \pi/2)$  or  $(R = a, \theta = \pi/2)$ . Because the Kerr solution is stationary, the circle on which the singularity lies is a geodesic. To investigate its velocity, it is assumed that  $r$  and  $\cos \theta$  are small,  $r^2$  is negligible and  $dr = d\theta = 0$ . The Boyer-Lindquist metric then becomes:

$$ds^2 = 2mr \frac{(a \sin^2 \theta d\phi - dt)^2}{a^2 \cos^2 \theta} \quad (\text{B.8})$$

As  $\cos \theta$  becomes infinitesimally small, to preserve  $ds^2 \leq 1$ , the numerator must converge as rapidly as  $\cos^2 \theta$  to zero, so the term within parentheses vanishes yielding

$$v_{\text{ring}} = R \frac{d\phi}{dt} = \frac{\sqrt{r^2 + a^2 \sin^2 \theta}}{a \sin^2 \theta} = 1 \quad (\text{B.9})$$

showing that the singularity travels with coordinate velocity  $c$  when  $a^2 > 0$ . This is to be compared with the coordinate velocity of particles and photons remaining on the equator of the Kerr BH event horizon but being dragged around with

the horizon. To investigate this, after setting  $dr = d\theta = 0$  and  $\theta = \pi/2$  the metric reduces to:

$$r ds^2 = (r - 2m)dt^2 + 4am dt d\phi - (r^3 + ra^2 + 2ma^2)d\phi^2 \quad (\text{B.10})$$

To remain on the horizon,  $ds^2$  is necessarily zero and the radius at the event horizon is given by  $r_+ = m + \sqrt{m^2 - a^2}$  so that  $R_+^2 = 2m(m + \sqrt{m^2 - a^2}) = 2mr_+$ . Solving for  $d\phi/dt$  allows the coordinate velocity of the equatorial event horizon to be determined:

$$v_{\text{eh}} = R_+ \left. \frac{d\phi}{dt} \right|_{r_+} = \left[ \frac{a^2}{2m(m + \sqrt{m^2 - a^2})} \right]^{1/2} \quad (\text{B.11})$$

which varies from  $v_{\text{eh}} = 0.5a/m$  as  $a \rightarrow 0$  to  $v_{\text{eh}} \sim 0.7a/m$  as  $a \rightarrow m$ . The Kerr-Newman metric endowed with charge  $Q$  features an outer event horizon at  $r_+ = M + \sqrt{m^2 - Q^2 - a^2}$  and, after restoring constants, remains sub-extremal if

$$G^2 m^2 \geq GQ^2 + c^2 a^2 \quad (\text{B.12})$$

so charge and rotation act repulsively and in unison to drive the BH away from spherical symmetry. This conclusion seems inevitable without abandoning the equivalence principle (Petkov, 2001), which in any case invalidates the metric. Since extremality cannot be surpassed, general relativity restricts static particles to having  $Q/M \leq \zeta_{\text{max}} = \sqrt{G}$ . Gross violations are witnessed in particle physics, for protons  $Q/M > 10^{13} \zeta_{\text{max}}$  and for electrons  $Q/M > 10^{16} \zeta_{\text{max}}$ . Besides quantum scales, this means that a tiny electrical charge can profoundly affect large-scale spacetime geometries. For instance, if an imbalance of one electron/proton exists for every  $\sim 10^{13}$  neutrons, the time dilation at the surface of a neutron star is almost entirely eliminated. Electromagnetism can thus play an important role in the stability of charged tori.

Consider a planar constellation of  $N$  identical satellites of total mass  $M$  evenly and symmetrically distributed on a circle (Fig. B.1). According to Newtonian mechanics, equilibrium is given by the balancing of gravitational and centripetal forces acting on each satellite such that the radius,  $r$ , of the circular orbits remains constant. All satellites rotate at constant angular velocity  $\omega$  so that their individual velocities are  $v = \omega r$ . Equilibrium is attained when:

$$\frac{GM}{4Nr^2} \sum_{n=1}^{N-1} \frac{1}{\sin(\frac{n\pi}{N})} = \frac{v^2}{r} \quad (\text{B.13})$$

In the limit  $N \rightarrow \infty$ , the series can be expressed in the form of a definite integral:

$$\lim_{N \rightarrow \infty} \frac{1}{N} \sum_{n=1}^{N-1} \frac{1}{\sin(\frac{n\pi}{N})} = \int_0^\pi \frac{dx}{\sin x} = \frac{4rv^2}{GM} \quad (\text{B.14})$$

Although the series converges for  $N < \infty$ , the integral is divergent since

$$\int_0^\pi \frac{dx}{\sin x} = \left[ \log \left| \tan \frac{x}{2} \right| \right]_0^\pi = 2 \times \lim_{x \rightarrow +0} \log \left( \frac{2}{x} \right) \quad (\text{B.15})$$

Hence, a ring of finite total mass  $M$  composed of an infinitude of individual satellites is obliged to rotate at infinite velocity in order to maintain radial equilibrium. This in turn implies an infinite angular momentum and kinetic energy for homogeneous rings. Planetary ring systems, such as Saturn's, are nevertheless observed. Despite their self-gravity, the rotational velocity remains modest – evidence

that their microscopic structure is particulate, not homogeneous. Where self-gravitating rings of matter are concerned, homogeneity is an unreasonable assumption, but one which is often adopted in general relativity as exemplified by the Kerr metric.

Some of the following statements are necessarily speculative, but it should be kept in mind that the overly complacent alternative is to trust in mathematical models when conditions are far more extreme than those accessible to experimental tests. Acceleration of the Kerr singularity to the speed of light formally requires an infinite amount of energy. This energy must have been supplied by the gravitational potential energy of the matter which the black hole consumes. It is implausible that this energy source is truly unbounded, allowing the spacetime to attain infinite curvature. Rather, the collapse must halt at some limiting density, at which time the kinetic energy remains finite. Therefore, though the Newtonian analysis presented is very simplistic, aspects of this simplicity are also shared by its relativistic counterpart, the Kerr black hole.

In an attempt to circumvent these limitations and prepare rough estimates, suppose that the ring structure is subdivided into a non-infinite number of satellites. For instance, the maximum number of neutrons contained in a mass of  $10^9 M_\odot$  is  $\epsilon^{-1} = 1.2 \times 10^{66}$ . In this case, the equilibrium satellite velocity remains finite with magnitude

$$v \approx \sqrt{\frac{GM}{4r} \int_{\epsilon}^{\pi-\epsilon} \frac{dx}{\sin x}} \sim 8.7 \sqrt{\frac{GM}{r}} \quad (\text{B.16})$$

But in these situations, neutrons are plausibly replaced by Planck-scale particles. The characteristic Planck length is  $l_p = \sqrt{\hbar G/c^3} \sim 1.6 \times 10^{-35} \text{m}$  and the Planck mass is  $m_p = \sqrt{\hbar c/G} \sim 2.2 \times 10^{-8} \text{kg}$ . A Kerr BH of mass  $M$  contains a singularity of maximal radius when  $a = M$  or  $R = MG/c^2$  in natural units. Suppose that the singularity is a crystalline structure of Planck ‘particles’ in a circular arrangement whose further collapse is resisted by quantum mechanical repulsion. One might object that this arrangement is too idealised or that it requires an infinite universal time to elapse - perhaps so, but it is here argued that some form of uncertainty principle or holographic correspondence prevents external observers from distinguishing between the present assumption and any other model. The mean separation between adjacent Planck particles is determined to be *independent of the total mass* and given by  $d_{\text{sep}} = 2\pi R m_p / M = 2\pi \sqrt{\hbar G/c^3} = 2\pi l_p$ , a coincidence substantiating the original premise of a Planckian singularity. For a  $10^9 M_\odot$  BH, the total number of particles is  $\epsilon^{-1} = 9 \times 10^{46}$  which yields  $v \sim 7.4 \sqrt{GM/r} = 7.4c$ . The equivalent relativistic velocity is  $\Gamma = 8.4$  or  $v_{\text{rel}} \sim 0.993c$  (for a stellar mass BH,  $v_{\text{rel}} \sim 0.992c$ ). It is known that the ratio  $a/m$  for a Kerr BH can realistically approach  $\sim 0.998$  in astrophysical circumstances (Thorne, 1974), allowing scope for deviation from the Kerr geometry due to Planck scale phenomena.

Though the margin for this to occur seems slender for isolated horizons, indicative of almost negligible deviation, the assumption that the singularity is quantum-mechanically sustained at the Planck scale introduces additional considerations which, in typical settings, are favourable for significant deformation of the Kerr geome-

try. The spacetime curvature in the vicinity of the singularity is tamed by the repulsion between Planck particles (e.g. Louko & Matschull, (2001) where some success has been claimed regarding the quantization of geometry). This repulsion presumably grows as the ring’s radius and  $a/m$  decreases. Whereas the Kerr singularity is infinitely distant from the black hole’s exterior due to the immensely strong curvature (Thorne, Price & MacDonald, 1986), the Planckian singularity is susceptible to the influence of other matter through tidal gravity. Indeed, the surface gravity of a Kerr-Newman BH diminishes with increasing charge and rotation, disappearing altogether at extremality. So without infinite curvature, the singularity would otherwise be deformable.

Most modern attempts at unification invoke extra spatial dimensions. At high energies, gravity is thought to ‘leak’ away from our 3 dimensions. This has yet to be confirmed experimentally, due to practical difficulties. Measurements have verified the inverse square law down to submillimetre scales, equating to an energy scale  $\sim 10^{-2} \text{eV}$ : well short of particle accelerator energies  $\sim 100 \text{GeV}$ , the supersymmetry scale  $\sim 10^{16} \text{GeV}$  and the Planck scale  $m_p c^2 \sim 10^{19} \text{GeV}$ . Diminution of gravitational interactions at small scales would inevitably cause the orbital velocities of BH singularities to decrease further, quite feasibly by a substantial amount. General relativity will certainly break down at the highest energies, otherwise collapse cannot even be halted at the Planck scale. Since energy conditions are known to be violated by the Casimir effect and Hawking radiation, it is unlikely that they will be satisfied everywhere within a black hole. Conversely, the extreme pathology of closed timelike curves exhibited by the stationary BH metrics is tacitly embraced by investigators.

Consider an accretion disk orbiting a rapidly rotating BH. The disk gravity induces tidal stresses on the Planckian singularity which tends to stretch it radially. In addition to the accretion disk, AGN reside within a molecular torus and host galaxy, each equatorially oriented with respect to the BH. In the context of rotary core collapse SNe, the outer shells collapse towards the plane of rotation where a substantial proportion of the debris forms a thick disk. Its mass and proximity to the core impose tidal forces whose influence on the central BH will be more pronounced than in AGN situations. The gravitational potential at radius  $r$  in the plane of a circular hoop of radius  $R \geq r \geq 0$  whose linear mass density is  $\lambda$  is given by the following function containing a complete elliptic integral of the first kind  $K(k)$ :

$$\Phi_{\text{hoop}}(r) = \frac{R}{r} \Phi_{\text{hoop}}\left(\frac{R^2}{r}\right) = -\frac{4G\lambda R}{R+r} K\left(\frac{2\sqrt{Rr}}{R+r}\right) \quad (\text{B.17})$$

$\Phi_{\text{hoop}}$  decreases monotonically from the centre ( $r = 0$ ) to negative infinity as  $r \rightarrow R$ . In elementary functions, it can be proven (by using series expansions for the elliptic integral and differentiating) that the internal ( $g_{\text{int}}$ ) and external ( $g_{\text{ext}}$ ) gravitational accelerations are bounded as follows:

$$\pi \leq \frac{(R^2 - r^2)g_{\text{int}}}{rG\lambda} \leq 4 \leq \frac{(r^2 - R^2)g_{\text{ext}}}{RG\lambda} \leq 2\pi \quad (\text{B.18})$$

The lower bound corresponds to  $r \ll R$ , the central limit to  $r \rightarrow R$  and the upper bound is the asymptotic behaviour as  $r \rightarrow \infty$ . These functions are readily integrated in many situations and permit the simple construction of models in which one may be interested in calculating conser-

vative estimates. For increased accuracy, interpolations are available whose maximum errors are  $\sim 0.2\%$  at  $r/R \sim 0.57$  for the internal gravity and  $\sim 0.9\%$  at  $r/R \sim 1.29$  for the external gravity, which is oppositely directed:

$$g_{\text{int}}(r) \approx G\lambda r \left[ \frac{4}{R^2 - r^2} - \frac{4 - \pi}{R(R^2 - r^2)^{1/2}} \right] \quad (\text{B.19})$$

$$g_{\text{ext}}(r) \approx G\lambda R \left[ \frac{4}{R^2 - r^2} - \frac{2\pi - 4}{r^{3/2}(r^2 - R^2)^{1/4}} \right] \quad (\text{B.20})$$

Of immediate interest are truncated disks of constant areal mass densities  $\sigma$ . Integration leads to the following approximation for the gravity within a thin truncated disk ( $0 \leq r \leq R_\alpha < R_\beta$ ) where  $R_\alpha$  and  $R_\beta$  are the disk's radii at the inner and outer rims respectively:

$$g \approx 2G\sigma \log \left[ \frac{(R_\alpha + r)(R_\beta - r)}{(R_\alpha - r)(R_\beta + r)} \right] - (4 - \pi)G\sigma \left[ \cos^{-1}\left(\frac{r}{R_\beta}\right) - \cos^{-1}\left(\frac{r}{R_\alpha}\right) \right] \quad (\text{B.21})$$

It is often assumed that BH accretion disks are truncated some distance from the event horizon because stable circular orbits are forbidden within  $r_{\text{ms}}$ , the innermost radius of marginal stability. For Schwarzschild BHs,  $r_{\text{ms}} = 6M$ , for retrograde extremal Kerr orbits,  $r_{\text{ms}} = 9M$ , and for prograde extremal Kerr orbits,  $r_{\text{ms}} \rightarrow M$ . Instability implies that material penetrating within these boundaries is accelerated towards the event horizon, so that these regions can scarcely be totally vacated. The acceleration experienced by infalling material, according to Newton's third law, is counterbalanced by a smaller but oppositely directed acceleration of the Planckian singularity towards the surrounding disk. When the singularity is teased towards larger radii, the BH is likely to accumulate further angular momentum. Hence, continued accretion and tidal distortion can reinforce the distortion, making it conceivable that nonstationary accretion into the event horizon, coupled with continuous disk replenishment, could maintain a TBH against collapse for prolonged periods. According to this view, a TBH might evolve from a spheroidal BH and vice versa — topological transitions of both kinds being possible. This enhances the probability of TBH formation, circumventing the need for collapse of a toroidal dust cloud or star as outlined in section 2. It also raises the question of whether the nuclei of some galaxies are revived into activity following a dormant stage e.g. by tidal interaction with nearby galaxies or more directly, following mergers. Elliptical galaxies, believed to be the outcomes of mergers, host an overabundance of AGN.

In conclusion, though Kerr's metric for rotating black holes is rightly celebrated as one of the landmark discoveries of 20th century science, the subsequent failure to satisfactorily unite the classical theory of general relativity with quantum mechanics remains a severe impediment to an understanding of nature. Until this fundamental obstacle can be overcome, one must be fully aware of the inherent drawbacks of myopic alternatives. Black hole topology is a subject unsuitable for purely classical computations, however sophisticated the mathematical veneer. Extreme caution should be employed if results are to be usefully construed. The rule of thumb calculations presented here are suggestive that an ultimate theory might accommodate the possibility of toroidal black holes, temporarily stabilised on astrophysically relevant timescales by the action of accretion, tidal deformation

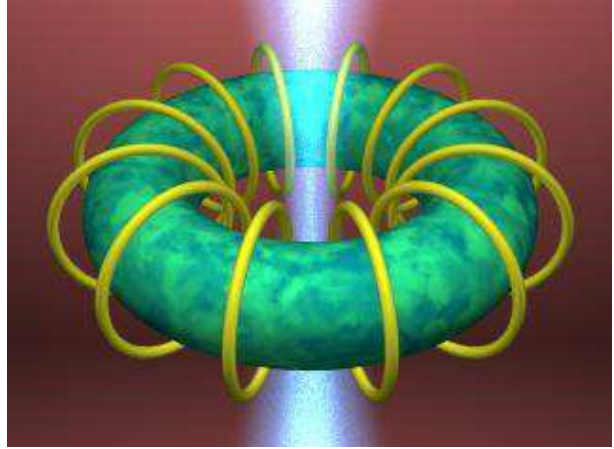


**Figure B.2.** Depiction of a rotating electrically charged torus exhibiting a dipole magnetic field in the non-rotating frame. The field lines channel plasma from a surrounding accretion disk into the central aperture where jets are outwardly accelerated along the spin axis by ergoregional interactions.

and Planck scale repulsion. The basis of the scenario advocated for supporting TBH stability is summarised below:

- Black holes will often be formed with nearly maximal rotation e.g. from collapse of moderately rotating stellar progenitors. Accretion via a thin disk can also lead to a rapid build-up angular momentum. Astrophysically realistic ratios of  $a/m$  can approach 0.998. Near-extremal black holes are therefore predicted to exist in rotary core-collapse supernovae, galactic nuclei and accreting black hole binary systems. In all situations, tidal stresses are exerted by matter exterior to the event horizon which orbits in the equatorial plane. Disk truncation decreases as extremality is approached, the radius of the innermost stable orbit and the singularity converge towards that of the event horizon. Mass steadily migrates into the event horizon by accretion, bridging the zone of disk truncation and bolstering the tidal forces acting on the singularity.

- The Kerr geometry is in some respects unphysical — it contains a homogeneous ring singularity rotating at the speed of light, infinite spacetime curvature at the location of the singularity, closed timelike paths within its Cauchy horizon and makes no provision whatsoever for quantum mechanics. Furthermore, all attempts to match the exterior metric with realistic non-vacuum internal distributions of matter have thus far failed.

- If collapse halts at the Planck-scale, the velocity of rotation could decrease to  $\sim 0.993c$ , suppressing the spacetime curvature in the vicinity of the singularity making it susceptible to tidal deformation by surrounding structures e.g. thin disks, thick disks and tori. High energy effects such as gravity 'leaking' into higher dimensions may additionally modify the rotational velocity of the singularity. Radial elongation of the Planck singularity is conducive to the accumulation of angular momentum beyond that of undistorted configurations, acting as a barrier against collapse should accretion be interrupted. Sustained accretion and tidal distortion *might* ultimately result in toroidal event horizon topology.